Advances from R2CA project on reactor simulations for burst rod number evaluation during LOCA

Sébastien Belon, Stefano Ederli, Matthias Jobst

Annals of Nuclear Energy 208 (2024) 110772

Contents lists available at ScienceDirect

Annals of Nuclear Energy

journal homepage: www.elsevier.com/locate/anucene

Advances from R2CA project on reactor simulations for burst rod number evaluation during LOCA

Sébastien Belon [a,*], Stefano Ederli [b], Matthias Jobst [c]

[a] Institut de Radioprotection et de Sûreté Nucléaire (IRSN), PSN-RES/SEMIA/LEMC, F-13115 Saint-Paul-Lez-Durance, France
[b] Agenzia nazionale per le nuove tecnologie, l'energia e lo sviluppo economico sostenibile, ENEA, Lungotevere Thaon di Revel, 76, 00196 Roma, Italia
[c] Helmholtz-Zentrum Dresden-Rossendorf e. V., HZDR, Bautzner Landstraße 400, 01328 Dresden, Deutschland

ARTICLE INFO

Keywords:
LOCA
Burst
Simulation
PWR
Fuel

ABSTRACT

In the frame of the "Reduction of Radiological Consequences of design basis and extension accidents" European Union's Horizon 2020 project, a specific effort was focused on the update and the development of methodologies to assess the radiological consequences of loss-of-coolant accidents. Evaluation of the radiological consequences associated to this accident is strongly linked to the prediction of the rod burst ratio and new approaches were investigated through research and development associated to accident simulation software. Complementarily to approaches chaining system thermalhydraulic simulation to fuel performance code, approaches with integral codes ASTEC, DRACCAR and ATHLET-CD were developed respectively by ENEA, IRSN and HZDR. These applications were demonstrated on LOCA simulation for PWR and highlighted the capabilities of the tools. The ASTEC PWR model was extended by ENEA, which proposes a 2D core model with an increased number of representative fuel rods. HZDR and IRSN proposes approaches based on 3D core model which are able to capture distinctive fuel assembly responses and predict the rod burst ratio according to the distribution of rod behaviors within the core. This work highlighted several possible core models to predict the rod burst ratio and which can be used in integral tools abled to couple thermal hydraulics and thermomechanics. Advanced core models simulating the thermomechanical response of several representative rods per fuel assemblies and using 3D thermal hydraulics model are recommended due to the heterogeneities on power distribution, which impacts flow distribution. The need to model RPV in 3D was underlined by ATHLET-CD large break loss-of-coolant demonstrative case, which exhibits non-symmetric core heat-up.

In addition, demonstrative cases proposed by ENEA and IRSN compared predictions obtained with the specific burst criteria developed in the frame of R2CA project and more classical one devoted to the core coolability assessment. The strong sensitivity of the rod burst ratio prediction to the burst criteria was highlighted. The need to handle uncertainties within a global methodology for rod burst ratio evaluation was underlined.

Abbreviations: APROS, Dynamic process simulation software developed by VTT Technical Research Centre of Finland Ltd; ASTEC, Accident source term evaluation code; ATHLET, GRS software: Analysis of THermal hydraulics of LEaks and Transients; ATHLET-CD, GRS software: Integral severe accident software based on ATHLET system thermalhydraulic software; CV, Control volume; CL, Cold leg of the primary circuit; DBA, Design basis accident; DEC-A, Design extension condition of type A: without core melt; DRACCAR, IRSN software dedicated to LOCA multi-rod simulation: Déformation et Renoyage des Assemblages Combustibles en Condition d'Accident de Refroidissement – translated: Deformation and reflooding of fuel assemblies in cooling accident conditions.; FA, Fuel assembly; ECCS, Emergency core cooling system; FRAPCON, Fuel performance code for the calculation of steady-State, thermal–mechanical behavior of oxide fuel rods for high burnup developed by Pacific Northwest National Laboratory for the U.S. Nuclear Regulatory Commission; FRAPTRAN, A computer code for the transient analysis of oxide fuel rods developed by Pacific Northwest National Laboratory for the U.S. Nuclear Regulatory Commission; GRS, Gesellschaft für Reaktorsicherheit; IB LOCA, Intermediate break loss-of-coolant accident; LB LOCA, Large break loss-of-coolant accident; LHGR, Linear heat generation rate; LOCA, Loss-of-coolant accident; LOOP, Loss-of-offsite power; PCT, Peak cladding temperature; PWR, Pressurized water reactor; PZR, Pressurizer – primary circuit component; R2CA, European union Horizon 2020 project: Reduction of Radiological Consequences of design basis and extension Accidents; RBR, Rod burst ratio; RC, Radiological consequences; RCS, Reactor coolant system; RIP, Rod internal pressure; RPV, Reactor pressure vessel; SA, Severe accident; SCRAM, Emergency shutdown of nuclear reactor; TFO, Thermo fluid object – specific object from ATHLET code; TRANSURANUS, Fuel performance code for the thermal, mechanical and neutron-physical analysis of a cylindrical fuel rod in nuclear reactors developed by Joint Research Center for the European Commission.

* Corresponding author.
E-mail address: sebastien.belon@irsn.fr (S. Belon).

https://doi.org/10.1016/j.anucene.2024.110772
Received 19 December 2023; Received in revised form 19 April 2024; Accepted 5 July 2024
Available online 11 July 2024

Finally, throughout the development of loss-of-coolant accident applications with ASTEC, DRACCAR and ATHLET-CD, some prospects of development were identified for the codes and should bring advances for LOCA simulation and RBR predictions.

1. Introduction on burst rod number evaluation during LOCA

1.1. Overview of LOCA simulation on failed rod evaluation methodologies

The evaluation of the radiological consequences associated to the design basis accidents (DBA) is a part of safety assessment for the pressurized water reactor (PWR) which should demonstrate that the requirements on radiation protection for these accidents are met (International Atomic Energy Agency. Vienna, 2016). In addition, the scope for radiological consequences evaluation was enlarged to the design extended conditions without core melt (DEC-A). Among accidents studied, loss-of-coolant accident (LOCA) which is initiated by a breach in the primary circuit belonging to the reactor coolant system (RCS), is characterised by a drop of primary coolant pressure and inventory causing a partial or full core uncovery. Therefore, the accident leads to the fuel rod heat-up and an increase of the difference between the rod internal pressure and the primary coolant pressure. In response to these conditions, fuel rod burst can occur accompanied by fission products release. This corresponds to the source term within containment, which must be evaluated prior to the prediction of the off-site radiological consequences.

Methodologies associated to the evaluation of the radiological consequences (RC) for the loss-of-coolant accident highly varies from one country to another. Indeed, these methodologies are linked to the design, the consideration on LOCA fault sequence and are also strongly influenced by the requirements imposed by national regulation. Therefore, radiological consequence evaluation methodologies can rely on conservative approach or on combination between conservative approach relaxed with more or less realistic description. The latter evolution was born from the progress in simulation tool and the need, mainly carried by the operators, to reduce the excess of conservatism. This was already a target at the end of the 20th century (Stephenson et al., 1991). In the frame of the Reduction of Radiological Consequences of design basis and extension Accidents (R2CA) European project (Reduction of Radiological Consequences, 0000), a specific review of methodologies used for radiological consequences assessment was handled among project participants. This review showed that the approach for radiological consequences assessment is decoupled from the core coolability demonstration and that the failed rod number is mainly assumed as an input for radiological consequences evaluation. Such assumption does not allow to measure the influenced on the failed rod number brought by the evolution of the fuel design or by the modification of safety systems or accident management procedures. To handle this issues, specific evaluation of the failed rod number is required.

Considering the progress brought to simulation tool for LOCA phenomena, the prediction of the failed rod number by simulation is promising for an evolution of RC methodologies for LOCA. Some researches were carried with fuel performance code chained to thermal-hydraulic system code (Adorni et al., 2011; Arkoma et al., 2015; Capps et al., 2021) to simulate LOCA phenomena and to predict rod failure. Existing application mainly consists in using a system thermal–hydraulic code which provides the thermal hydraulic conditions, which are applied as boundary conditions for single rod simulation. Then a single fuel rod simulation evaluates the fuel rod thermomechanical behavior and the burst occurrence. In general, the possible feedback of the thermomechanical response of the fuel rod on the crossflows or on the neighboring rods is only partially considered in such method. In the R2CA European project, a specific research effort was focused on the update and the development of methodologies based on simulation tool to assess the radiological consequences of loss-of-coolant accidents within DBA and DEC-A conditions. In particular, the use of integral tools coupling thermal hydraulics to thermomechanics and using realistic 3D core descriptions were investigated.

1.2. R2CA main objectives and activities for failed rod number evaluation in LOCA conditions

The Reduction of Radiological Consequences of design basis and extension Accidents (R2CA) is a European Horizon 2020 project which included specific focus on the update and the development of methodologies to assess the radiological consequences of loss-of-coolant accidents within DBA and DEC-A conditions. In support to this methodology, specific research was carried on simulation of the system reactor transient and on source term prediction. This research work included the development of new modelling approaches for LOCA based on integral software abled to couple thermal hydraulics to thermomechanical phenomena. The main objective is to propose some evaluation of the failed rod number, which can either be used to predict radiological consequences or to quantify gain brought by design evolution or mitigation systems.

To assess the failed rod number, two distinctive approaches were used in the frame of R2CA project. The first one consists in evaluating system thermal hydraulic response with a system thermalhydraulic code (such as RELAP5, ATHLET or APROS) and chain its results to a fuel performance code (such as TRANSURANUS or FRAPTRAN). Such calculation chain decouples the system thermalhydraulic analysis of the fuel rod behavior simulation. However, due to the fast-running capabilities of fuel performance code, it allows to describe behavior of large number of fuel rods by running numerous single rod simulations. This approach is similar to the one used in (Adorni et al., 2011; Arkoma et al., 2015). The second approach consists in an integral approach, which couples thermal hydraulics to thermomechanics within the same application and based on improved or advanced core models. In the frame of the project, ENEA investigated the capabilities of the severe accident code ASTEC using an extended 2D core ring model. In addition, specific 3D core modelling coupled to system description of reactor circuits were respectively developed by HZDR with ATHLET-CD and by IRSN with DRACCAR. All these three integral approaches aim at improving the core description in order to predict with more accuracy the number of burst rods during LOCA. These approaches are depicted in the following sections and are illustrated by demonstrative case simulations. The obtained results cannot be directly used for PWR safety assessment as it corresponds to research work using demonstrative cases. Through this work, different core models are investigated, and in particular advanced 3D core models are proposed for LOCA simulation.

Simultaneously with the development of these methods, some outcomes from R2CA project were obtained on burst prediction and were experimented with simulation tools. Indeed, the knowledge acquired on cladding behavior in loss-of-coolant accident was reviewed with the objective to propose prediction of burst with an improved accuracy. Experimental results from burst experiments including separate effect tests and semi-integral tests were gathered and specific burst criteria were fitted on burst stress and burst temperatures. If new criteria were proposed (Taurines and Belon, 2022), no available criterion was found to predict with accuracy both the burst timing and the burst strain. Therefore, for burst risk assessment, burst criteria which predict with confidence the burst timing were recommended. Depending on the approach and the need, various criteria were proposed which are more or less envelope of the experimental burst results. In addition, to cover

the various conditions associated to LOCA transients, burst stress and burst temperature criteria were proposed.

In support to the development of these new burst criteria, the criteria were tested to evaluate rod burst ratio on demonstrative cases using updated modelling approaches developed in the project. The evaluation from these criteria were compared by some partners to the response obtained with criteria classically used for LOCA analysis devoted to core coolability assessment such as burst strain from NUREG-0630 (Powers and Meyer, 1980). Some results from this comparison are highlighted here after for the three depicted integral approaches.

2. Upgraded ASTEC code integral application

The main features of ASTEC code are described in the following section.

2.1. ASTEC code description

The ASTEC integral code (Accident Source Term Evaluation Code) models the main phenomena which occur during severe accident (SA) sequences in water cooled reactors (Chatelard, 2016). In a single simulation, it is possible to characterize: the reactor coolant system (RCS) thermalhydraulic response (CESAR module) and the fuel rod thermal behaviour and degradation (ICARE module); the release of fission products (ELSA module) from fuel as well as their transport in the RCS and containment (SOPHAEROS module); the discharge of radionuclides elements into the environment (CPA module). The latter representing the Source Term (ST) for the estimation, with dedicated codes, of radiation exposure outside the Nuclear Power Plant (NPP).

All simulations presented in the paper were performed with the 2.2.0.1 version of the code.

2.2. ASTEC modelling of reactor

The simulated reactor is a generic PWR 900 MWe with three primary and secondary loops and a thermal power of about 2800 MW. The description of ASTEC modelling is mainly focussed on core configuration and criteria adopted for the fuel cladding bursts.

2.2.1. Nodalization

The starting point for the ASTEC modelling was the input-deck developed by IRSN during the past EU-CESAM project (Chatelard, et al., 2017; Nowack et al., 2018), the reactor core being simulated with 5 groups of fuel rods contained in 5 radial fluid channels. Such core model was developed for SA applications, characterized by large extent of core melt and degradation and it could be not accurate enough for the estimation of failed fuel rods number and FPs release in the case of Design Basis Accidents (DBA) and Design Extension Condition Accidents, without significant core degradation (DEC-A), which are analysed within R2CA.

After the application of the above-described core setup for the first set of reactor calculations, performed at the beginning of the project, it was decided to improve the core modelling by considering a higher number of fuel rod groups in each of the 5 fluid channels. The number of fluid channels was kept unchanged because a refined radial discretization using ring shaped channels is not advisable, being the thickness of fluid channels close to the size of a FA (approximately 25 cm).

The core modelling setup was then established looking at the distribution of decay heat in the 157 FAs of the generic PWR-900 that (Fig. 2.1) is the main parameter driving the core radial thermal behaviour during the accidental transient. All groups of fuel rods in each fluid channel are then subject to the same fluid conditions (temperature, pressure, void fraction…) but distinguished by different decay heats. It is worth noting that the decay heat is automatically computed by ASTEC (ISODOP module) from the considered FPs mass inventory, therefore, there is no differences between the radial distribution of decay heat and

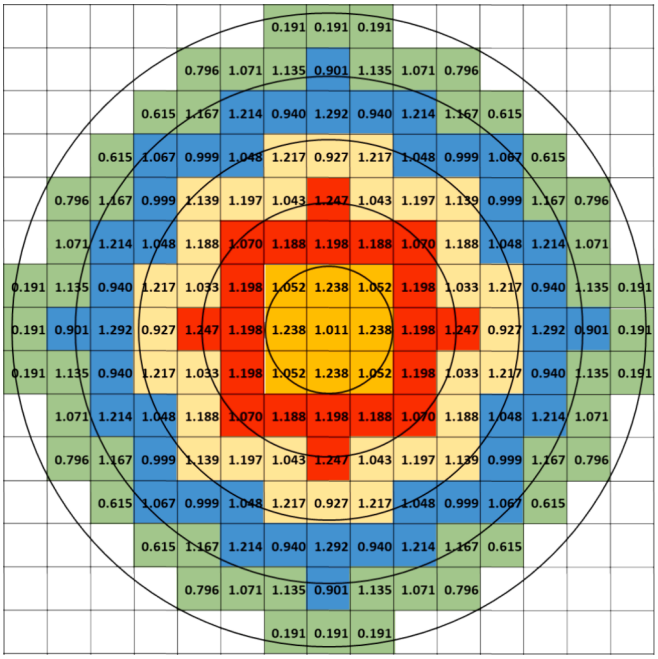

Fig. 2.1. Horizontal map of decay-heat distribution in the core and radial fluid channels.

FPs mass and, often in the paper, it will be referred indifferently to decay heat radial factors or FPs mass inventory radial factors. Moreover, at this time, ASTEC uses the total FP inventory which is distributed on all groups of fuel rods according to its FPs total mass inventory radial factor.

The following rules were adopted to define the number of fuel rod groups in each fluid channel:

- A minimum of 2 representative fuel rods are defined to simulate respectively the FAs characterized by maximum and minimum decay heat.
- The remaining FAs are lumped into a maximum of 3 more representative fuel rods by grouping together FAs with similar decay heat. Basically, FAs having a decay heat factor within one of the 3 ranges of power below are lumped into a single representative fuel rod with averaged decay heat.

$f_{min} < f \leq 0.95$.
$0.95 < f \leq 1.08$.
$1.08 < f < f_{max}$.

f is the decay-heat factor of the generic FA while f_{min} and f_{max} are respectively the minimum and maximum decay heat factor considered in fluid channel.

The adopted method leads to define a total of 20 groups of fuel rods distributed within the 5 fluid channels, as reported in Fig. 2.2 together with the decay heat radial factors of each group of fuel rods and the number of FAs represented. Representative rods are identified as "ROD" plus 2 numbers; the first one indicates the radial fuel channel where representative rods are positioned and the second one indicates, in decreasing order of decay-heat, the different groups of fuel rods in the channel.

It must be stressed that the map of decay heat distribution reported in Fig. 2.1 is just a coarse approximation of the real distribution expected at the end of cycle, in the case of ¼ core re-loading strategy of the reactor. Moreover, the assumed distribution of neutronic power only depends on the radial fuel channel where the groups of fuel rods are enclosed (i.e., all representative rods of a given fluid channel are characterized by the same neutronic power) and the imposed pressure, at room temperature, is the same in the 20 groups of fuel rods.

Fluid Channel	Representative fuel rod	Weight (N° of FAs)	Decay heat radial factor
1	ROD11	4	1.238
	ROD12	4	1.052
	ROD13	1	1.011
	3 Rep. Rods	9 FAs	
2	ROD21	4	1.247
	ROD22	12	1.195
	ROD23	4	1.070
	3 Rep. Rods	20 FAs	
3	ROD31	8	1.217
	ROD32	12	1.175
	ROD33	8	1.038
	ROD34	4	0.927
	4 Rep. Rods	32 FAs	
4	ROD41	4	1.292
	ROD42	8	1.214
	ROD43	20	1.032
	ROD44	8	0.940
	ROD45	4	0.901
	5 Rep. Rods	44 FAs	
5	ROD51	8	1.167
	ROD52	8	1.135
	ROD53	8	1.071
	ROD54	16	0.706
	ROD55	12	0.191
	5 Rep. Rods	52 FAs	
Total N° of Rep. Rods = 20		Total N° of FAs = 157	

Fig. 2.2. Upgraded CORE modelling with 20 groups of fuel rods in 5 radial fluid channels.

Considering the above-mentioned limitations, the presented simulations must be only intended as demonstrative applications of proposed methodology and core setup in ASTEC code. Of course, correct and accurate enough boundary conditions are a prerequisite to perform realistic analysis of the core thermo-mechanical behavior.

The nodalization of whole reactor (vessel, primary and secondary side of RCS) is illustrated by Fig. 2.3.

2.2.2. Criteria for cladding burst

The failure of fuel claddings is simulated by considering a main burst criterion (EDGAR (Chailan et al., 2019; Pettersson, 2009) or CHAPMAN (Powers and Meyer, 1980; Chailan et al., 2019) can be selected) combined with two other criteria that are: a simple user criterion defining the maximum hoop strain (default value = 40 %) above which the cladding failure is assumed and the NUREG 630 criterion[1] (Powers and Meyer, 1980; Chailan et al., 2019).

Some of burst correlations adjusted by IRSN within the R2CA project (Taurines and Belon, 2022) were moreover implemented in ASTEC code to be used as main burst option instead of EDGAR or CHAPMAN (Chailan et al., 2019). The two types of burst criteria used are:

- True burst stress criteria formulated as exponential law on temperature. These criteria belongs to the family of burst correlations of the true stress vs. cladding temperature (as EDGAR criterion) with general expression: $\sigma_{burst} = k.e^{-q.T}$, with T the cladding temperature and couple (k,q) some parameters obtained by fitting experimental results. Several values for these parameters were proposed in (Taurines et al., 2023) considering a Best-Estimate exponential function fitting the experimental results (BE-exponential) and various envelopes: Min, Mean and Max. The correlations are established for heating rate in the range from 1 to 20 °C/s.
- Burst temperature criterion correlating burst temperature to the engineering stress and heating-rate (as the correlation proposed by Chapman (Powers and Meyer, 1980; Chapman, 1979). In this work, the R2CA temperature criteria from (Taurines and Belon, 2022), and described in (Taurines et al., 2024) and in section 3.2, was used.

In performed simulations, the cladding failure is then triggered by the first criterion, which is fulfilled between the selected main burst criterion and the defined maximum cladding hoop strain.

2.3. Short description of simulated accidental scenarios

The DBA scenario is initiated by an intermediate break of 16.3″ in the cold leg (CL) of a primary loop without pressurizer (PZR) when the reactor is at nominal power. An additional penalty is the Loss Of Off-site Power (LOOP) at the reactor SCRAM and the failure of one emergency diesel generator leading to losing one of the two trains of the safety injection system. The accident is automatically managed in agreement with standard procedures of French PWRs.

The DEC-A scenario is initiated by a small break of 4″ in the hot leg of a primary loop without pressurizer when the reactor is at an intermediate subcritical hot state when the reactor residual power is approximately 1 % of the nominal power, the primary pressure is roughly 70 bar and the average water temperature in the primary loops is about 236 °C (509 K). The accumulators are disabled and the Emergency Core Cooling System (ECCS) is manually started after 36.5 min from the accident onset.

2.4. Numerical results

The discussion of results is focused on the estimation of failed fuel rods number with the above-described core modelling and selected burst criteria.

2.4.1. DBA scenario

Five simulations were performed by adopting the burst criteria adjusted by IRSN combined with a maximum hoop strain of 40 % (default value). An additional simulation was made with BE-exponential stress criterion and a reduced maximum hoop strain (25 %).

In the simulations with default maximum hoop strain (40 %), cladding failures are observed only if Min burst stress or burst temperature criteria are selected. The other criteria are never fulfilled, and maximum hoop strain remains below the threshold of 40 %. Fig. 2.4 illustrates the evolution vs. time of maximum fuel cladding temperature in the 20 representative rods when the Min burst criterion is applied. The different groups of fuel rods in the fluid channels are identified by the names reported in Fig. 2.2. The temperature differences between the fuel rods positioned in the same fluid channel are in general very small, suggesting that their thermal behavior is mainly driven by the thermal hydraulic conditions in the fluid channel. Only in the outermost fluid channel can be observed a significant temperature difference (more than 50 K) between the hottest and coldest group of fuel rods that are characterized by very different decay heat radial factors (Fig. 2.2).

The timing of fuel cladding failures is well indicated by the sudden drops of fuel rods internal pressures (Fig. 2.5) until a value matching the primary pressure. The first cladding failure is observed in the hottest group of fuel rods (ROD21) of fluid channel 2 (51 s) and, after approximately 64 s from the accident onset, all the fuel rods contained in the first four fluid channels, representing the 66.88 % of the total, are burst (Table 2.1). Only the five groups of fuel rods in the outermost fluid channel remain intact.

The failure margins, for the 4 burst criteria based on true stress vs. cladding temperature, are given by the difference between the burst stress and computed true stress in the cladding of a given representative

[1] Finally, the NUREG 630 strain criterion was disabled in all performed simulations because, in some cases, it was reached during the cooling of fuel rods while such a criterion, consisting in two correlations depending on the claddings heat up rate, should be applied only during the heating of the fuel rods, according with the experiments used for its formulation.

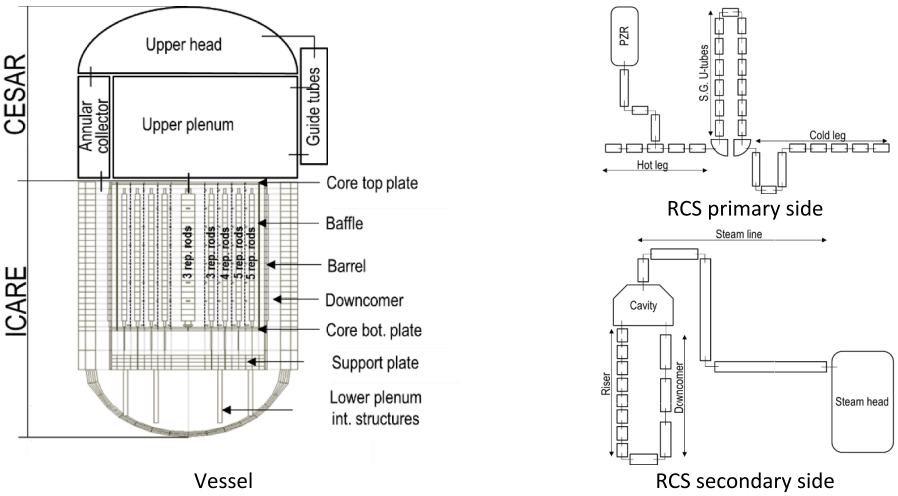

Fig. 2.3. Reactor nodalization.

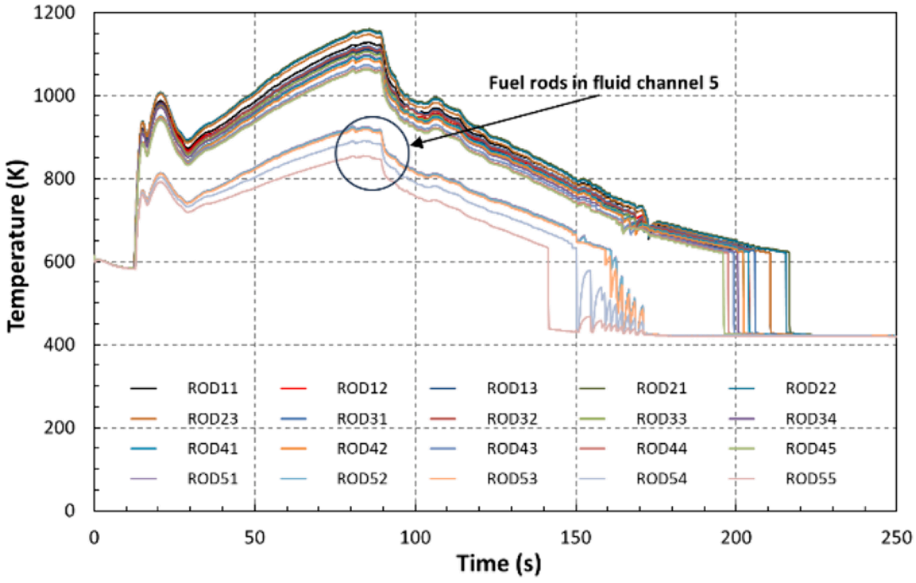

Fig. 2.4. Maximum fuel cladding temperatures vs. time with Min burst criterion and maximum hoop strain = 40 % (DBA).

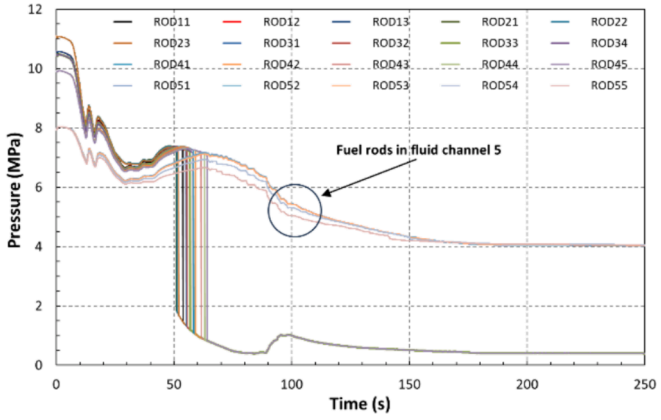

Fig. 2.5. Internal fuel rods pressure vs. time with Min burst criterion and maximum hoop strain = 40 % (DBA).

Table 2.1
Number of failed fuel rods (DBA).

Main burst criterion	Max. clad hoop strain (%)	Number of failed fuel rods (% of the total)	Time of first cladding failure (s)
True stress BE-exponential	40	0	/
True stress BE-exponential	25	12.74 (*)	80.6
True stress Mean	40	0	/
True stress Min	40	66.88	51.0
True stress Max	40	0	/
R2CA temperature	40	66.88	56.9

(*) Failure triggered by the fulfilment of maximum allowed hoop strain.

fuel rod. Fig. 2.6 shows the evolution vs. time of such a difference for the hottest fuel rod of fluid channel 2 (ROD21) and for the four mentioned burst criteria.

The curves plotted in the Fig. 2.6 confirm that only Min stress envelope is reached (margin to this burst criterion becomes 0 after 51 s

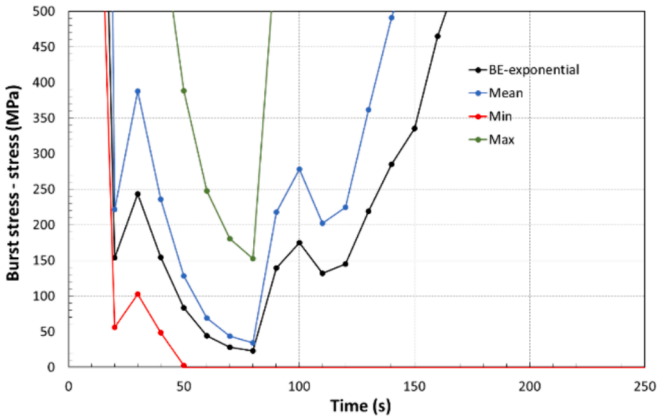

Fig. 2.6. Difference between burst stress criterion and computed cladding true stress in the ROD21 (DBA).

from the accident beginning). The margin to the burst criteria of BE-exponential and Mean stress envelopes are not significantly different while a larger distance Max engineering stress envelope burst criterion is observed (~150 MPa).

The application of R2CA temperature criterion leads to the failure of the 66.88 % of all fuel rods in the core, as obtained with the Min burst stress envelope. The difference between burst temperature and computed cladding temperature is a measure of the margin to burst for the R2CA temperature criterion. The evolution vs. time of such a quantity, again for the ROD21, is shown in Fig. 2.7. In this case the cladding failure occurs after ~ 57 s from the transient beginning that is slightly later than what observed in the simulation with Min burst criterion suggesting that R2CA temperature criterion is a somewhat less conservative criterion, although the same number of failed fuel rods is estimated for the accidental scenario considered (Table 2.1).

The reduction of maximum allowed hoop strain (25 % instead of 40 %), in the simulation with BE-exponential main burst criterion, leads to the failure of all fuel rods in the fluid channel 2, corresponding to the 12.74 % of the total that is much lower than what computed with Min envelope on burst stress and R2CA burst temperature criteria (Table 2.1).

The effect of improved core model is basically irrelevant for the simulated accidental scenario considering that, in all calculations, the representative rods in each fluid channel all fail or, conversely, all remain intact.

2.4.2. DECA-A scenario

Fig. 2.8 illustrates the evolution vs. time of maximum fuel cladding temperature, predicted with the BE-exponential burst criterion, in the 20 representative fuel rods. The quite high core temperatures that characterize the simulated accident, lead to a greater deformation by creep of fuel claddings than in DBA scenario and the maximum allowed hoop strain of 40 %, triggering the claddings failure, is reached in all fuel rods contained in the first four fluid channels, corresponding to the 66.88 % of the fuel rods in the core. This is proved by the evolution of claddings hoop deformation showed in Fig. 2.9. The same results are observed in the simulations with Mean and Max criteria meaning that in such cases the selected main burst criterion is completely irrelevant for the estimation of failed fuel rods number (Table 2.2).The five burst criteria adjusted by IRSN were again applied combined with a maximum hoop strain of 40 %.

The simulation with R2CA burst temperature criterion predicts the same number of failed rods (all fuel rods in the first four fluid channels corresponding to the 66.88 % of the total) but, in such a case, the fuel rod failures are caused by the R2CA temperature criterion itself, that is

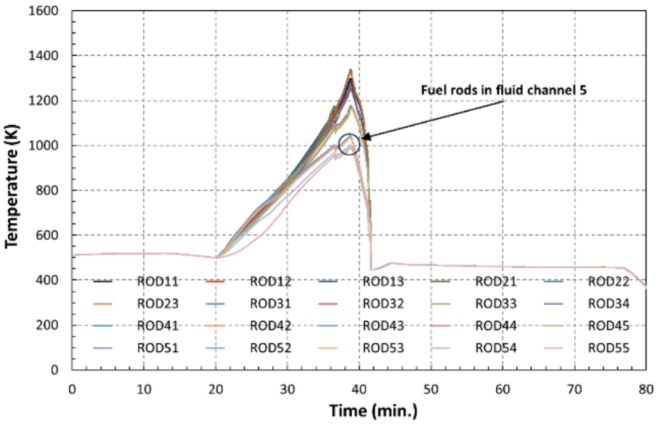

Fig. 2.8. Maximum fuel cladding temperatures vs. time with BE-exponential burst criterion (DEC-A).

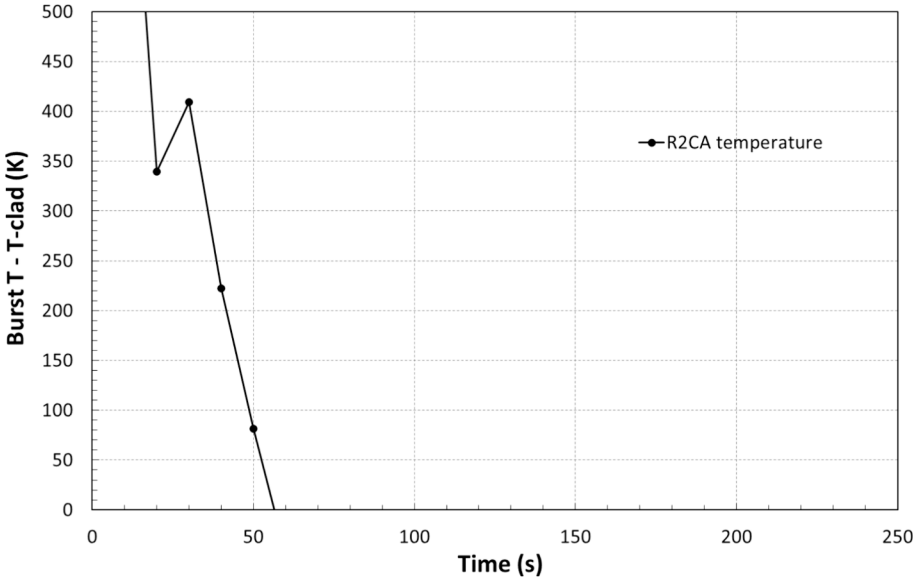

Fig. 2.7. Difference between burst temperature and computed cladding temperature in the ROD21 (DBA).

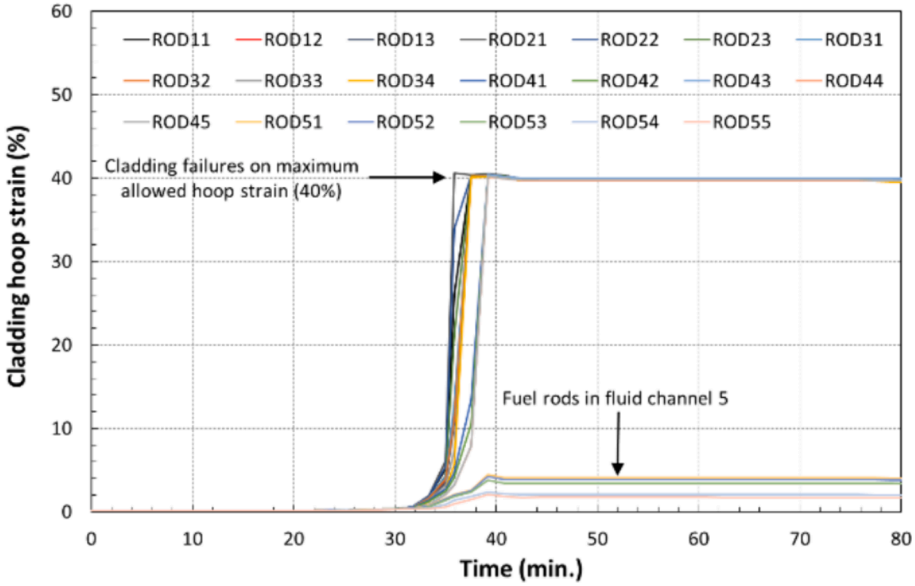

Fig. 2.9. Fuel claddings hoop strain vs. time with BE-exponential burst criterion (DEC-A).

Table 2.2
Number of failed fuel rods *(DEC-A)*.

Main burst criterion	Max. clad hoop strain (%)	Number of failed fuel rods (% of the total)	Time of first cladding failure (min)
True stress BE-exponential	40	66.88 (*)	35.86
True stress Mean	40	66.88 (*)	35.86
True stress Min	40	71.97	33.93
True stress Max	40	66.88 (*)	35.86
R2CA Temperature	40	66.88	34.64

(*) Failure triggered by the fulfilment of maximum allowed hoop strain.

fulfilled earlier in the transient (Table 2.2), when the fuel claddings hoop strain is much lower than the maximum allowed value of 40 %. It must be also stressed that the margins of ROD51 and ROD52 in fluid channel five are not very comfortable, as the difference between computed and burst temperature is less than 50 K (Fig. 2.10).

In the simulation with Min stress burst criterion, the cladding failures involve all fuel rods in the first four fluid channels plus a group (ROD51) contained in the fluid channel five, as showed by Fig. 2.11 where one can observe that also ROD52 and ROD53 are close to the failure. Of course, such fine description of the thermo-mechanical behavior of fuel rods would be impossible with only a representative rod in each fluid channel demonstrating, in such case, the added value of upgraded core modelling. The number of failed fuel rods estimated with Min stress burst criterion is the 71.97 % of the total (Table 2.2).

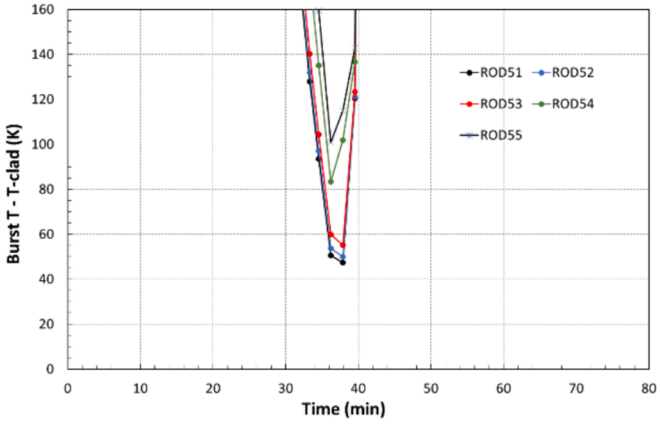

Fig. 2.10. R2CA temperature criterion, burst T – computed T in the fuel rods of fluid channel 5 (DEC-A).

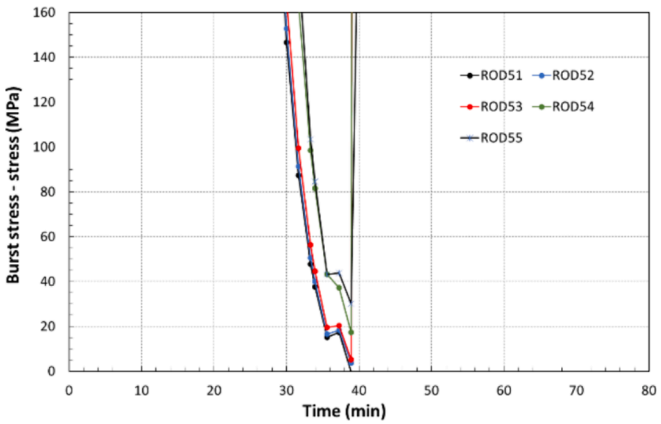

Fig. 2.11. MIN criterion, burst stress – computed stress in the fuel rods of fluid channel 5 (DEC-A).

2.5. *Discussion of ASTEC results*

The upgraded core modelling, considering 20 representative fuel rods distributed within 5 radial fluid channels, has been successfully applied to the ASTEC simulations of DBA and DEC-A scenarios in a generic PWR 900 MWe. The implemented core modelling allows to predict the failure of only a portion of the fuel rods located in each fluid channel. Such update of core model would improve the accuracy of estimation compared to the use of a single fuel rod per ring. Nonetheless, most of obtained results show that the thermo-mechanical behavior of the fuel rods is mainly driven by thermal–hydraulic conditions meaning that, in a given fluid channel, all fuel rods fail or all remain intact (practically the same result would be obtained with the simple model considering only one representative fuel rod for each fluid channel). The partial failure of fuel rods in a fluid channel was observed only in a simulation of DEC-A. In such a case, the failure involved the fuel rods of

outermost fluid channel characterized by very significant differences on the distribution factor of decay heat, ranging from 1.167 in the hottest group of fuel rods to 0.191 in the coldest one.

It must be stressed that presented simulations only intend to demonstrate that the proposed core modelling can be properly adopted in ASTEC applications. Therefore, further calculations, with more realistic and accurate boundary conditions (power and pressure distribution in the fuel rods), will be needed to draw reliable conclusions on the added value of proposed core modelling for estimating the number of failed fuel rods.

In DBA scenario, the estimated number of failed fuel rods ranges between 0 to 66.88 % of the total, depending on the selected burst criterion and the user options on maximum allowed claddings hoop strain. The effect of burst criteria seems to be less relevant in the case of DEC-A scenario. Such a results can be however misleading because in the case of less conservative burst criteria (i.e. BE-exponential, Mean and Max stress envelopes) all fuel rod failures are triggered by the fulfilment of maximum allowed hoop strain, while the main burst criteria are never reached. It must be also stressed that, at the present, ASTEC code doesn't manage the possible contact between neighbouring fuel rods, therefore it cannot be reliably applied in case of too large cladding deformations. The default value of 40 % is already a little bit too high considering that, in a PWR, the contact between adjacent fuel rods is possible for deformation greater than 33 %. This is an important limitation of the code for design extended conditions accidental scenarios, characterized by high fuel temperatures and cladding deformations as well as for demonstration of core coolability in loss-of-coolant accident analysis.

3. Advanced DRACCAR LOCA integral application

Within R2CA project, IRSN developed a specific approach to evaluate the radiological consequences of LOCA based on a simulation chain between DRACCAR LOCA software (Glantz et al., 2018) and ASTEC integral code (Chailan et al., 2019). DRACCAR software is mainly devoted to study LOCA for multi-rod configuration at a subchannel scale. The classical DRACCAR model focus on a single fuel assembly at subchannel scale coupling thermal hydraulics and thermomechanics to depict the relation between rod ballooning and flow blockage which directly affects the fuel assembly coolability. In the frame of R2CA, DRACCAR application scope was extended to reactor system simulation. A specific DRACCAR PWR model was developed to depict the core and RCS circuits able to simulate core response to LOCA and evaluate the associated RBR.

3.1. Description of new DRACCAR reactor application for RBR evaluation

Regarding the objectives for RBR evaluation and considering the possible heterogeneities of the core loading map – and so of the characteristics of fuel assemblies composing the core which can influence thermomechanical behavior of the fuel rods – it was considered that each fuel assembly should be represented distinctively to estimate its fuel rods potential for burst. This consideration is reinforced when the core is designed with a pattern mixing fuel types such as mixed (UO2, MOX) core loaded in the French 900MWe PWR. However, due to the current computation performance, simulation of the whole core at subchannel scale depicting each fuel rod is not achievable with DRACCAR. Indeed, it requires to represent several tens of thousands of subchannels and fuel rods in 3D configuration. Consequently, a compromise between the description details and the computation performance was selected.

The proposed DRACCAR PWR model consists in a 3D core thermal hydraulics element connected to 0D/1D RCS elements – distinguishing each loop and modelling primary and secondary sides. In the R2CA demonstrative application, the system thermal hydraulics during LOCA is resolved in the whole fluid domain by the IRSN code CESAR, embedded in DRACCAR software. The 3D core description uses one fluid channel per fuel assembly discretized in 40 axial levels in the core active zone. Therefore, core channels are interconnected and forms a 3D thermal hydraulics core model in which both axial and transverse flows are evaluated. In each core channel, the corresponding fuel assembly is described by some weighted structure objects describing fuel rods, control rods or spacer grids. In particular, the thermomechanical behavior of fuel rods is evaluated using 2D (r,z) equivalent rod object coupled to an average fuel assembly thermal hydraulics. Even if the fuel rods are not described using DRACCAR 3D (r,θ,z) detailed fuel rod object, most of the DRACCAR physical models are still applicable to 2D (r, z) equivalent rod object. The main differences between the DRACCAR RCS model using 2D (r,z) fuel rod objects and a classical DRACCAR 3D detailed assembly model are summarized in the Table 3.1. With equivalent rod object, the coupling between thermal hydraulics and thermomechanics is still realized by DRACCAR even if the thermal hydraulics is not solved at subchannel scale but averaged at fuel assembly scale. Such core description with DRACCAR was considered to be the best compromised to depict the heterogeneities of core loading map and save the computation performance. The IRSN demonstrative case did not use full 3D RPV model with 3D meshed vessel plenums since the 3D core domain is connected to 1D/0D volumes representing vessel plenums. As a 3D model is not used to distribute flow to the different hot legs and as the considered core loading map is symmetrical, the core could be fractioned in eighth. Such a simplification leads to use only 26 core channels (1040 meshes) instead of 157 (6280 meshes) for this PWR demonstrative case. This simplification speeds significantly the simulation, which are mainly impacted by thermal hydraulics resolution cost. Indeed, the 300 s of the demonstrative DBA simulation costs several months of CPU when using full core DRACCAR model (157 fuel assembly channels) and that time is reduced by a factor of 20 – less than few days – when modelling only the eighth of the core. The lack of description associated to this simplification is partially balanced by the gain on CPU cost since it allows to perform a large number of simulations necessary for uncertainty analysis. The Table 3.1 reminds the main characteristics of the DRACCAR model used by IRSN in the frame of updated demonstrative reactor applications task of the project.

To depict the initial state of the core before LOCA, the proposed method relies on data and plant design completed by simulation results using neutronic and fuel performance code (Fig. 3.1). Specific attention was paid to the respective initial state of fuel rods, which can directly influence the rod response during LOCA such as the geometry, the burnup, the power, the rod internal pressure, the initial temperature field or the oxide layer thickness. These data are gathered for each fuel assemblies and accounting for fuel type $(U,Pu)O_2$ or UO_2 as well as rod power factor (representing stored energy) and decay heat (associated to fission products rod inventory).

Then the scenario and the plant behavior are represented by DRACCAR using the core and the RCS model which depicts initiator, normal and safety systems operation. The simulation predicts the rod response for each equivalent rod and evaluate the occurrence of burst by the reach of burst criteria. The fission product gap inventory is released burst-by-burst and feed some specific boundary condition of the chained ASTEC application, which is able to compute fission gas transport and behavior on the same CESAR thermal hydraulics nodalization of RCS.

3.2. DRACCAR demonstrative application

3.2.1. Scenario

The demonstrative case focus on a 900MWe alike pressurized water reactor. The design basis accident scenario selected consists in 16.3 in. intermediate break located on the cold leg of a primary loop without pressurizer. Initial power is 104 % of nominal power. In addition to break, the loss-of-offsite power occurs at SCRAM and due to emergency diesel failure, only one high pressure and one low pressure safety injection lines are available. Successively to the accident initiation, rapid

Table 3.1
Main characteristics of the DRACCAR core & RCS model developed for R2CA and classical DRACCAR 3D PWR fuel assembly model.

Features	DRACCAR core & RCS model proposed in R2CA	Classical DRACCAR 3D detailed 17x17 PWR FA model
Description scale	Core (assuming symmetries) + RCS minimum: 1/8th of core = 26 FA	Fuel rod sub-channels1 FA described in detail
Core / FA meshing	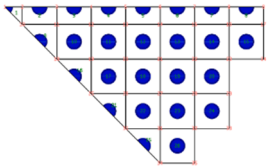 8th of core	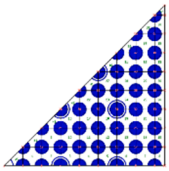 8th of FA
Fuel assembly description	Average 2D model At least 1 equivalent fuel rod, 6 were considered in demonstrative case 1 equivalent control rod + guide tube 1 equivalent instrumentation tube 8 spacer grids + support grid	1/8th FA Detailed 3D model 39 fuel rods 5 control rods & guide tubes1 instrumentation tube 8 spacer grids
Fuel rod description	Equivalent rod model 2D (r,z) thermal meshing Creep: 2.5D (θ,z) clad contour	3D detailed rod model 3D (r,θ,z) thermal meshing Creep: 2.5D (θ,z) clad contour
Fuel rod axial discretization	At least 40 axial slices	
Cladding azimuthal discretization	1 thermal node At least 40 mechanical nodes	At least 3 to 4 thermal nodes At least 40 mechanical nodes
Fuel rod heat transfer modelling	3D (r,θ,z) conductive heat transfer including at contact between rods Wall-to-fluid convective heat transfer including 2-phase flow regimes, reflooding model and accounting for ballooning and contact Simplified FA to FA radiation heat transferbased on effective conductivity of FA	Rod-to-rod radiative heat transfer accounting for deformation, shading or contact (based on Hottel method)
Fuel heat generation	Normal power evolution (rod power factor, axial profile, time evolution) Decay Heat from time evolution law (rod power factor, axial profile, time evolution) or from FP isotopes decay (evaluated by ISODOP module) Relocation of fuel associated to mass and energy transfer within fuel rod	
Thermomechanical modelling	2.5D (r,θ,z) secondary creep model with contact detection (Norton-law for creep rate + phase transformation) **New burst criteria specific to burst risk assessment (developed in the frame of R2CA)** Advanced phenomenology: gas transport within fuel rod, fuel relocation 90° rotational symmetry of clad contour over the rod axis Contact management: non-circular clad contour if radius exceeds rod pitch	Non-axis-symmetrical deformation Rod-to-rod contact management Impact of azimuthal thermal gradients
Core thermal–hydraulic description	3D 2-phase flow model with implicit coupling to thermal-mechanics T/H codes: CESAR^{IRSN} or CATHARE-3^{CEA}	
Core thermal–hydraulic channels	1 channel per FA Same axial discretization as for fuel rods (40 axial levels)	45 sub-channels
RCS thermal–hydraulic description	Full RCS model using thermal hydraulics 1D system description for circuits T/H codes: CESAR^{IRSN} or CATHARE-3^{CEA}	Boundary conditions from system code RCS simulations
RPV modelling	3D core domain 1D downcomer 0D lower and upper vessel plenums	3D core domain only
FPs release	evaluated for each FA – Evolution from initial FP isotopes total inventory of the core computed by ISODOP module and release evaluation from ELSA module ISODOP average core isotopes inventory is taken from VESTA depletion simulation	
Automatic chaining to source term evaluation tool	Chained to ASTEC simulation with FP transport and release modelling based on the same RCS description	No (Since no RCS is modelled)

depressurization of the RCS is observed until containment pressure is reached at nearly 75 s. Consecutively to the depressurization, saturation conditions are reached in reactor coolant system and a first core heat-up, strongly driven by core stored energy and power transferred to coolant and loss at break, is observed from 10 s. The primary mass decreases until the start of the hydro-accumulators discharge at nearly 40 s. As a large part of the core is uncovered, a second and progressive heat-up of the core is pursued mainly due to the decay heat. After 100 s when the hydro-accumulators are empty, the core water mass inventory is only progressively recovered by low pressure safety injection which refloods the core. A maximum peak cladding temperature of nearly 1000 K is reached at 150 s. Such PCT remains enough low to avoid massive burst of the fuel rods.

3.2.2. Core initial state and DRACCAR associated core model

The core considered in that PWR900 MWe alike case is a mixed fuel core composed of 56 mixed oxide $(U,Pu)O_2$ and 101 UO_2 fuel assemblies. Assuming symmetries, only 26 FAs are described in the DRACCAR core model to depict the behavior of the 157 FAs. Each of this fuel assembly is associated to a thermalhydraulic channel and to six different equivalent rods associated to a power factor taken from Table 3.2.

To manage heterogeneities of fuel assembly characteristics (Fig. 3.2), fuel performance simulations with FRAPCON4-0 (Geelhood et al., 2015) are run to depict irradiation state of each equivalent rod selected in DRACCAR core model. Additionally, the IRSN VESTA depletion core simulations are used to complete neutronic data on fuel assemblies especially neutron power, decay heat and the initial detailed fission products isotope inventory. Due to the large number of data, a specific procedure was developed to post-process and feed DRACCAR input

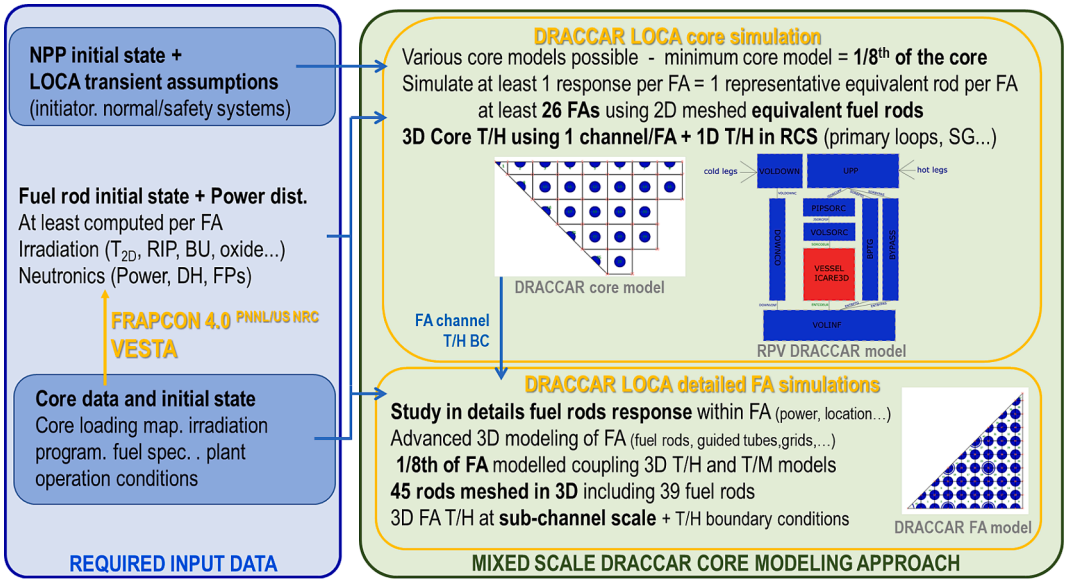

Fig. 3.1. DRACCAR PWR application for LOCA simulation with 3D core and multi 1D/0D RCS model.

Table 3.2
Rod power factor distribution considered in the fuel assembly.

Q0 – Minimum	0,920
1st quartile Q1	0,968
Average	1
Median Q2	1,018
3rd Quartile Q3	1,033
Maximum Q4	1,048

parameters, which depicts the fuel rod initial characteristics and set it in the 3D core model.

DRACCAR software is able to manage different rod power distribution for each FA. Indeed, this modelling is needed as the power distribution within FA is linked to the FA characteristics (burn-up, location in the core) and their design especially for complex UO2/PuO2 mixed FA, which are composed by rod with distinct Pu concentrations (Yamate et al., 1997). However, in the presented demonstrative case, the assumed power distribution among fuel rods in a given fuel assembly was considered the same for all fuel assemblies. This fictitious distribution was voluntarily selected to exhibit the influence of rod power on mechanical response to LOCA.

For each fuel assembly, each rod power factor from Table 3.2 plus the average power factor are attributed to a distinct equivalent rod. So, each fuel assembly is described using six different equivalent rods which depict the behavior of the fuel assembly rod population. Of course, as the DRACCAR core model use only one channel per fuel assembly, thermal hydraulics conditions are averaged for the different equivalent rods from the same fuel assembly. Wall-to-heat exchanges and thermo-mechanics are nonetheless particularized to each equivalent rod.

3.2.3. Burst criteria selection

In the frame of R2CA, an adequate selection of burst criteria for rod burst assessment was identified as a key issue. Thus, IRSN reviewed experimental data available on cladding burst in conditions representative of LOCA (Taurines and Belon, 2022; Taurines et al., 2024). From this work, even if no criterion able to predict simultaneously and with accuracy the burst timing and the burst strain was identified, new burst criteria for Zr alloy claddings were proposed specifically for rod burst prediction. A burst temperature criterion based on engineer stress was recommended for burst risk assessment in LOCA conditions. The R2CA temperature criterion is given by:

$$T_{burst}(^{\circ}\mathrm{C}) = \mathrm{A} - \frac{\mathrm{B}\,\sigma_{e,\theta}}{1 + \frac{\min\left(\frac{dT}{dt},38\right)}{C} + \mathrm{D}\,\sigma_{e,\theta}}$$

with A = 1145.2 °C, B = 188.5 kpsi^{-1}, C = 16,5°C/s and D = 0.335 kpsi^{-1}.

and where T_{burst} is the burst temperature (°C), $\sigma_{e\theta}$ the engineering hoop stress (kpsi) and $\frac{dT}{dt}$ the heating rate (°C/s). This model is only valid for heating ramps from 1 to 38 °C/s.

In addition to this criterion, the burst temperature proposed by Chapman (Powers and Meyer, 1980; Chapman, 1979) was also used in the IRSN demonstrative simulation. Moreover, to manage complex LOCA transients, in which burst can occur during the reflooding phase associated to strong variations of the cladding temperature and rod internal pressure, additional criteria were used complementarily to burst temperatures. Moreover, the burst strain criteria based on NUREG-630 (Powers and Meyer, 1980) and the "best-estimate" true burst stress criterion proposed by (Taurines and Belon, 2022) were also considered. As for ASTEC simulations, a circumferential strain limit is also set to prevent excessive deformation without burst when no criterion is reached. In fact, these three last criteria were not triggered in DRACCAR demonstrative simulations. Indeed, according to the transient conditions, the temperature burst criteria were triggered long before the conditions for other criteria were met (Fig. 3.3) and strain level remained low (3 % for DBA, 8 % for DEC-A demonstrative cases).

3.2.4. Discussion on main results

In this demonstrative DBA case, the maximum temperatures are nearly 1000 K for the hottest fuel assemblies (See Fig. 3.4). The cladding temperatures remain low enough to only observe burst for a reduced number of fuel rods (<10 %) and a low circumferential strain (<3%). Concerning burst predictions, a large scattering of the minimum distance between criterion and cladding representative parameters is observed. Burst occurrence is only predicted by the burst temperature criteria with a good agreement between Chapman and the new criterion proposed by Taurines. The code evaluation remains far of the criteria based on burst stress or strain (See Fig. 3.5).

Moreover, the distance between maximum clad temperature and the burst temperature varies a lot from one fuel assembly to the other. As the burst criteria act as a trigger for failed rod number, the burst potential of

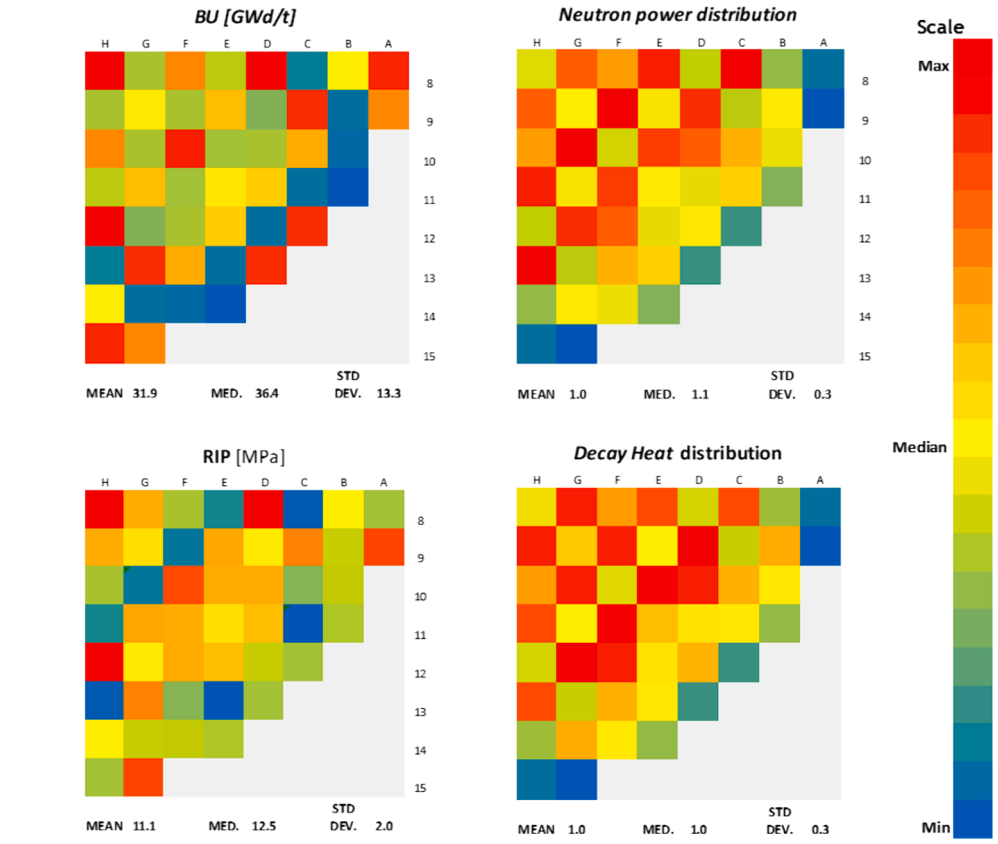

Fig. 3.2. Core loading map characteristics considered and average rod initial state for PWR900 alike demonstrative case.

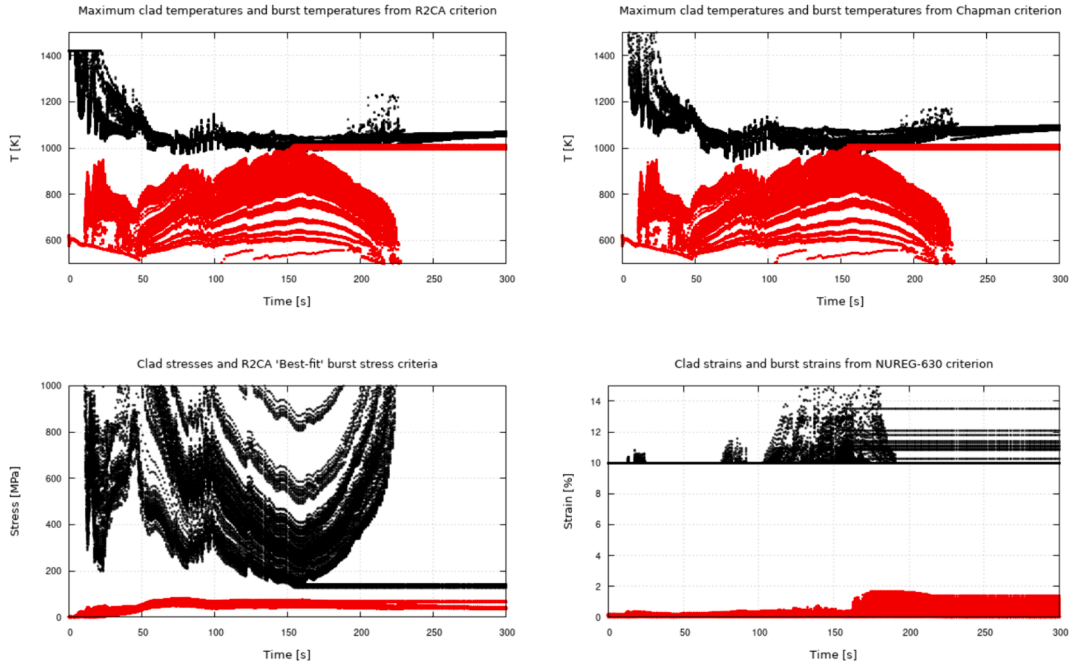

Fig. 3.3. Evolution of the value associated to clad elements (in red) and burst criterion (in black) for the selected criteria (temperature, strain, stress). (For interpretation of the references to color in this figure legend, the reader is referred to the web version of this article.)

each fuel rod was evaluated at a given time by the minimum relative burst margin which is the relative difference to burst criteria evaluated for each elements composing the cladding.

$$Min[(Value_{criterion} - Value_{code})/Value_{criterion}]$$

In particular, for a burst temperature criterion, this minimum margin can be evaluated for a given rod and at a given instant by the minimum reached over all the clad elements:

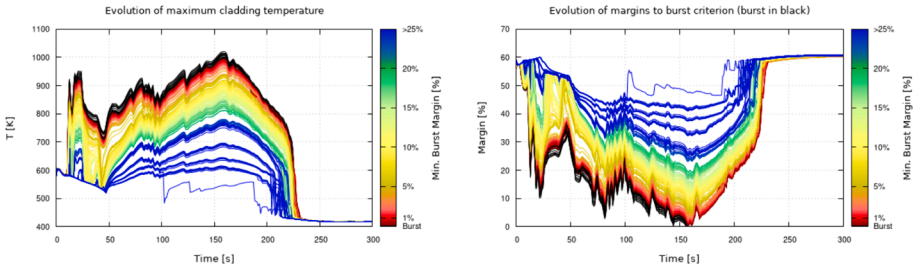

Fig. 3.4. Evolutions of the maximum clad temperatures (at left) and the relative margin between clad temperature and burst criterion (at right) – colour field represents minimum relative burst margin.

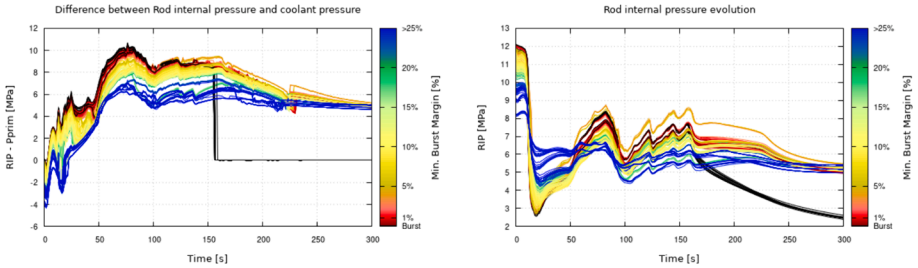

Fig. 3.5. Evolution of the difference between rod internal pressure and coolant pressure at burst location (at left) and of the rod internal pressure at mid elevation (at right) – colour field represents minimum relative burst margin.

$$Min_{\forall cladelementi \in rod}\left[\frac{T_{crit}(T_i,\sigma_i)-T_i}{T_i}\right]$$

With T_i the temperature of clad element i belonging to the fuel rod

T_{crit} the temperature criteria evaluated according to temperature T_i and stress σ_i for the clad element i belonging to the considered fuel rod.

For a given rod, the lowest value reached during the transient by the minimum margin corresponds to the conditions where the rod is closest to the burst criterion. Therefore, for a given rod, these conditions are associated to the maximum burst risk. This margin can be evaluated for each fuel assembly and for the six equivalent rods representing this fuel assembly. The minimum margin reached during transient is illustrated on the core map (Fig. 3.6). On this core map, the response of equivalent rods with minimum, average, median, and maximum power factors are identified for each fuel assembly. As expected, DRACCAR predicts burst for high power fuel assembly and preferentially for maximum power factor rod. Due to the use of burst temperature criteria and according to the characteristics of the demonstrative transient, the burst margins decrease monotonically with rod power factor.

Burst occurs preferentially in the fuel assembly with the maximum average power and with the highest rod internal pressure. In this simulation, burst temperature are met only for the hottest rods and during the reflooding phase when the cooling has already started at the bottom of the core. For the other of fuel rods, the temperature rise is cut-off before the cladding temperatures reach the burst temperatures. However, low margins to burst (<5%) are evaluated for a non-negligible amount of fuel assemblies.

The evaluation of minimum burst margin for the different equivalent rod was used to quantify the rod burst ratio in a fuel assembly by cumulating the burst frequency step-by-step from the response of equivalent rods using different power factors. This demonstrative method evaluates the RBR in a given fuel assembly to 25 %, 50 %, 75 % and 100 % when the burst is respectively predicted for the equivalent rod with maximum, third quartiles, median or first quartiles power factor. Core RBR is obtained by summing contribution of the different FAs. The obtained RBR was compared to the one deduced from the single response of one of the four family of equivalent rods respectively associated to minimum, maximum, median or average power factors. Fig. 3.6 illustrates this comparison by presenting the predicted RBR against the minimum relative margin to burst criteria. Results highlight the dependency of the RBR evaluation to the choice of the fuel assembly modelling and to the uncertainty magnitude on the clad and the burst temperatures. This simulation shows a strong variation of RBR with the minimum relative margin to burst. RBR jumps from 10 % to 30 %

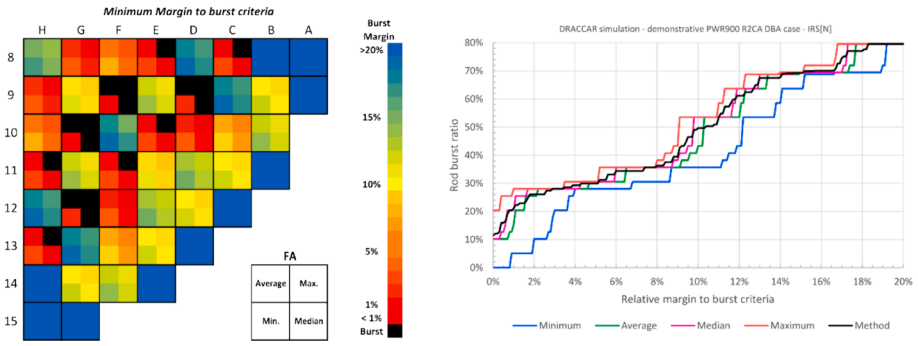

Fig. 3.6. Potential number of burst fuel rods predicted by DRACCAR against the threshold relative margin to burst criteria considering different equivalent rod population depending on rod power: average, maximum, minimum, median or a method accounting for different rod behavior.

considering that burst occurred with relative margin to burst lower than 5 %, which in this case roughly corresponds to 50 K between clad temperature and burst criterion. As a result, it is recommended that RBR evaluation should not rely on a single simulation and that a specific management of uncertainties, and in particular on burst criteria, should be included in the methodology. Indeed, due to dispersion of experimental data, the R2CA temperature criterion was established by a fit to data with a mean error of 26.7 °C (Taurines and Belon, 2022).

The obtained results are influenced by DRACCAR fuel rod model and especially by the evaluation of the rod internal pressure. In this example, no specific fission gas release from fuel to rod free volume was computed during the transient. It means that only the initial free volume inventory of fission gas is released at rod bursts. The inventory of fission products is deduced from the average isotope inventory evolution evaluated by ISODOP module and release is cumulated by ELSA module (Chatelard, 2016). These ASTEC modules are embed in DRACCAR software and ease connectivity of DRACCAR results to ASTEC simulation for source term evaluation. One current limitation of DRACCAR simulation is the use of the total core fission product inventory, which is distributed to the different representative rods according to their power factors. One prospect for the development in ISODOP module would be the management of several fission product inventories. In this way, the fission products and gas composition within free volumes could be defined independently for each rod according to its fuel design, burn-up and irradiation history.

Regarding the rod pressure evaluation, the demonstrative DRACCAR simulation uses axially meshed free volumes with specific gas transport model. Indeed, this modelling was considered according to the selected transient where burst occurs during reflooding. From the start of rod bottom reflooding, a uniform rod internal pressure assumption led to a rapid drop of pressure and so of the stress in clad even for the hottest rods. Consequently, uniform rod pressure assumption tends in this case to reduce the burst risk. Assuming local internal pressure with a gas transport model provide significant differences since the pressure can evolve with delays in response to start of the rod cooling from the bottom. One dimensional axial gas flow through the rod free volumes is computed by DRACCAR according to a classical porous media approach based on Darcy law. Therefore, the pressure differential between rod and coolant varies axially during the transient and at clad burst, the pressure is automatically set to coolant pressure at burst location whereas it can last few hundred seconds to upper plenum pressure to drop to the coolant pressure. With 1D axial gas transport model, the rod pressure distribution and evolution strongly depend on the axial equivalent permeability considered in Darcy's law. In this demonstrative case, rod initial permeability is taken to 10^{-14} m^2. This value is consistent with the order of magnitude characterized in (Montgomery and Norris, 2019). Of course, this parameter is uncertain and should be particularized to each fuel rods or at least to each fuel assemblies. Indeed, it can be noticeably influenced by fuel design and irradiation history. Moreover, permeability was not yet characterized in LOCA transient conditions. Consequently, in a rod burst assessment methodology, uncertainty management approach should certainly identify the permeability among other uncertain parameters, which are able to affect the simulation of rod response to a LOCA.

For few fuel assemblies, burst is not reached even with high pressure difference at burst elevation between the rod and the coolant pressure. For these rods, the power is insufficient to reach the temperature for burst. In this demonstrative case, the power factors (stored energy and decay heat) drive mainly the cladding thermal response, which primarily plays the major role in burst prediction due to the selection of burst temperature criteria.

3.3. Summary and prospects for DRACCAR application

In the frame of R2CA, IRSN has proposed new approach with DRACCAR LOCA software in which DRACCAR core model depicts distinctively the behavior of each fuel assemblies using a 3D core description based on average fuel assembly thermalhydraulic channels and several 2D (r,z) equivalent rods per fuel assembly. This 3D core model enclosed in multi 1D/0D RCS thermalhydraulic description efficiently evaluates the system thermalhydraulic response to LOCA for PWR and is coupled to thermomechanical models able to distinctively evaluate contribution of the different fuel assemblies to RBR.

RBR evaluation with DRACCAR was highlighted on a demonstrative PWR case, which is an example of simulation that could feed a global approach to assess the radiological consequences during LOCA. From this work, the choice of burst criterion was found to influence the RBR and burst temperatures criteria were reached earlier than classical NUREG-0630 burst strain or the "best-estimate" true stress criterion from R2CA project. The scenario and LOCA transients plays probably a role in burst criteria adequate selection and it is recommended to enable several types of criteria (stress, strain, strain energy density, temperature,…) among which burst temperature criteria from Chapman (Powers and Meyer, 1980) and from R2CA project (Taurines and Belon, 2022).

In addition, the prediction of the number of failed fuel rods should not rely on a single simulation result even with integral 3D simulation tools. Indeed, a specific management of uncertainty should be included in the methodology due to the uncertainty magnitude on inputs for the scenario or on the model parameters. This work underlines that the uncertainties attached to clad temperature predictions or burst criteria especially during reflooding conditions could impact significantly the RBR evaluation. Of course, uncertainty management should be considered globally for the calculation chain. It should handle the uncertainties for LOCA thermal hydraulics simulation and in particular on input model uncertainty (Baccou et al., 2019). Moreover, the chain to results from fuel performance code which provides the rod initial irradiation state associated to advanced fuel rod modelling such as gas transport model or fission gas release should also be dealt in uncertainty quantification. This probably implies a significant computational effort associated to a large number of simulations with a proper classification and selection of first order parameters for RBR evaluation.

Currently, using a reduction of the core domain to an eighth or a fourth of the core − as used in this DRACCAR demonstrative case − fit with the requirement on computational performance needed to perform these large number of simulations but at the expense of the representativeness. In particular, the proposed DRACCAR eighth core model cannot capture 3D in-vessel flow effects and non-symmetrical behavior of fuel assemblies. Moreover, non-symmetric core loading can only be represented rigorously by a higher computational effort. Some prospects associated to the improvement of numeric are investigated in DRACCAR software such as the use of optimized solver and methods such as the one available in PETSc (Balay et al., 0000). The reduction of CPU cost could allow to develop full 3D RPV model or to mesh the core at an intermediate scale in between fuel assembly scale and sub-channel scale. Of course, 3D model and in particular with multi-scale model would require verification and validation process before introducing it in industrial method for rod burst prediction.

The new DRACCAR core application represents with more realism the core in comparison to classical core ring methods used in integral tools such ASTEC. However, some compromised were realized on the meshing due to computational capabilities or on the physical description by the use of 2D(r,z) rods instead of the classical 3D (r,θ,z) multi-rod configuration at subchannel scale recommended with DRACCAR for LOCA phenomena studies. Since the current application mix realistic description and modelling compromise, a particular attention should be paid to the evaluations and conclusions based on simulation results. Even if DRACCAR approach describes with more realism the core, one should take care that the remaining conservatisms associated to rod burst prediction are not weakened by the attempt to introduce more realism in the modelling. This probably means to adopt some conservative approach managing simulations with penalizing assumptions and adding additional margins. The method should also handle correctly the

input and model uncertainties which can impact the evaluation of maximum rod burst ratio.

4. Advanced 3D ATHLET-CD application

In the framework of the R2CA project, a new 3D model of a PWR reactor pressure vessel (RPV) and core was developed with the system code ATHLET and its extension ATHLET-CD. The model was developed exemplarily for a 4-loop PWR of the Siemens KWU type (called Konvoi), with nominal 3950 MW thermal power and net electric power of 1400 MW. The plant model developed in the framework of the current work is generic with no reference to a specific plant, and all data is taken exclusively from open literature. Details about the type of plant can be found in (Neeb, 1997; E.ON, Kernkraftwerk Isar 2, 2011; von Linden et al., 2002; Ziegler and Allelein, 2013).

4.1. ATHLET and ATHLET-CD code description

The analyses were performed with the system code ATHLET, version 3.3 (Austregesilo et al., 2021) and its extension ATHLET-CD for modelling core-degradation phenomena (Lovasz et al., 2021). ATHLET is a best-estimate one-dimensional thermo-fluid dynamics code for simulation of large range of thermal–hydraulic systems with the focus to nuclear reactors applications. It applies a two-fluid model and solves six balance equations for both steam and liquid phase by means of a finite volume method, based on a fully implicit treatment of a first order upwind, donor-cell approximation of the fluxes on a staggered spatial grid by means of the ODE solver FEBE. The ability to solve the momentum equation in 3D-domains, such as RPVs, was introduced into ATHLET version 3.0A back in 2012 (Schöffel, 2011), with further improvements made in version 3.1A in 2016. Since that time, the 3D option has been applied for various light water reactor thermal hydraulic analyses (Diaz-Pescador, 2023). The validation of ATHLET's 3D capability was based on the recalculation of selected experiments (Diaz-Pescador et al., 2020; Diaz-Pescador et al., 2021; Pandazis et al., 2015).

ATHLET-CD is a predefined plug-in for ATHLET and extends the underlying ATHLET models and inputs with additional modules for the simulation of severe accident phenomena and processes (Wielenberg et al., 2019). In particular, it provides a core and fuel rod model, which is able to calculate the heat-up and deformation of fuel rods, calculation of gas-gap pressure, creep, deformation of cladding (ballooning) and burst of fuel rod cladding and reduction of the flow cross-sectional areas between the fuel rods (feedback to the thermal hydraulics). Furthermore, it provides the calculation of fission product inventory, decay heat, fission product release and transport within the primary circuit (Lovász et al., 2021). However, many of the ATHLET-CD features, such as melting and relocation of fuel rods are not needed for the current analyses of a DBA LB-LOCA.

The classical approach applied in severe accident codes such as ATHLET-CD is subdivision of the core into a small number of concentric rings with the assumption of azimuthally symmetric behavior, especially symmetrical power distribution and symmetrical thermal–hydraulic boundary conditions. A flexible nodalization scheme has been implemented in ATHLET-CD version 3.3 (Lovasz et al., 2021; Lovász et al., 2021), which provides several options of a more detailed nodalization of the core, including the possibility of a free definition of rectangular shaped nodes within a Cartesian coordinate system (applied in the current study). The new nodalization approach has been applied to accident analyses with strongly asymmetrical characteristics of the reactor core (Lovasz et al., 2018; Lovasz et al., 2018) as well as accident studies in spent fuel pools (Lovasz et al., 2018; Lovasz et al., 2019).

All analyses shown in the current paper were performed with a developer version of the code provided by code developer GRS with additional code modifications implemented by HZDR.

4.2. New detailed model of PWR reactor pressure vessel and core

The RPV is modelled by a hydraulic multichannel approach, i.e. the thermal–hydraulic domain of the RPV is subdivided azimuthally into inter-connected parallel channels. These channels are represented in ATHLET by so-called thermo-fluid-objects (TFOs) and each TFO is subdivided axially into a certain number of control volumes (CVs). Adjacent channels are interconnected by so-called cross-connection objects (CCOs), which provide flow paths between adjacent CVs. This 3D core model is widely inspired from ATHLET-CD 3D model developed for spent fuel pool configuration (Pointer et al., 2018).

Fig. 4.1 shows the nodalization scheme of the vessel, visualizing the described parallel channel approach. The downcomer for instance is modelled by in total 16 parallel channels (where only 2 are shown in Fig. 4.1), and the plena regions are modelled by 49 parallel channels, arranged in 3 concentric rings, each subdivided into 16 channels and one central channel.

The core region of the Konvoi PWR consists of 193 fuel assemblies (FAs), arranged by a 15-by-15 matrix, and each assembly comprises 300 fuel rods (57900 in total). For the new core model, it was decided to model each assembly separately with one TFO per assembly. This results in the scheme shown by Fig. 4.2 with 193 TFOs to model the FAs. The colors in the figure indicate which of the assemblies are connected to which part of the lower and upper plenum (with orange as the central fuel assembly, yellow connected to the 1st ring, green connected to the 2nd ring, and blue connected to the 3rd ring). The objects marked in grey indicate the reflector channels.

It has to be emphasized, that a model limited to the core alone or the RPV is not sufficient to study the plant behavior during LOCA accident, as precise boundary conditions at the RPV inlets and outlets are not known à priori. There is an interaction between the vessel and the loops and the emergency core cooling system (ECCS), e.g., the start of injection depends on how fast the pressure is reduced in the RPV.

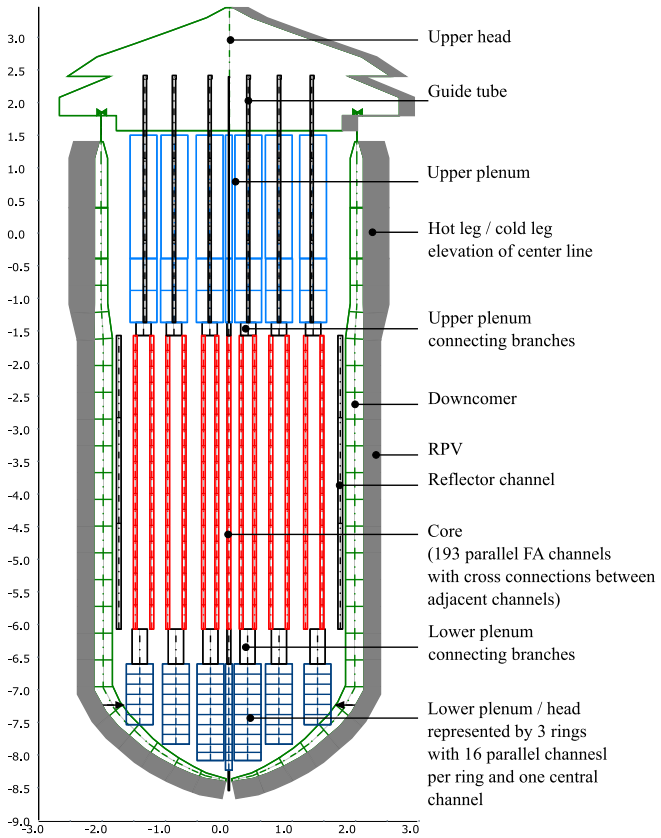

Fig. 4.1. Nodalization scheme of RPV.

0	0	0	0	204	204	204	204	205	205	205	205	206	0	0	0	0
0	0	203	203	203	160	161	165	166	167	173	174	206	206	206	0	0
0	202	203	154	157	158	159	162	163	164	171	172	179	180	207	207	0
0	202	152	153	155	156	63	64	68	69	169	170	177	178	187	207	0
202	202	149	150	151	58	59	62	67	73	74	168	175	176	186	207	208
201	145	146	147	148	56	57	61	66	71	72	78	79	183	184	185	208
201	142	143	144	53	54	55	60	65	70	75	76	77	84	181	182	208
201	140	141	49	50	51	52	7	8	9	80	81	82	83	192	193	208
201	138	139	45	46	47	48	4	5	6	85	86	87	88	190	191	209
200	136	137	41	42	43	44	1	2	3	12	13	14	89	188	189	209
200	134	135	40	37	38	39	34	29	24	19	10	11	94	95	96	209
200	131	132	133	35	36	32	33	28	23	17	18	90	91	92	93	209
200	199	129	130	128	122	30	31	27	22	15	16	100	101	102	194	194
0	199	125	126	127	120	121	25	26	20	21	108	109	98	99	194	0
0	199	199	123	124	118	119	113	114	115	105	106	107	97	195	194	0
0	0	198	198	198	116	117	110	111	112	103	104	195	195	195	0	0
0	0	0	0	198	197	197	197	197	196	196	196	196	0	0	0	0

Fig. 4.2. Detailed core configuration (location of 193 fuel assemblies with assembly numbers and assignment to core rings).

Furthermore, the reactor shows a strong asymmetric behavior during the LOCA transient:

- break of only 1 of 4 loops,
- asymmetric ECCS injection due to malfunction and outage of selected systems,
- influence of pressurizer, which is connected to only one of the loops.

Therefore, it was decided to develop the new core modelling approach within a full plant ATHLET model (including full primary and parts of the secondary circuits). Fig. 4.3 shows the nodalization scheme of the complete model, including:

- the RPV,
- 4 separate loops with hot leg, steam generator (SG) inlet and SG exit chamber, SG U-tubes, cold leg and main coolant pump (only 2 of the 4 loops are shown in Fig. 4.3),
- 1 pressurizer with surge line connected to hot leg of Loop #2,
- 8 accumulators (4 connected to hot legs, 4 connected to cold legs),
- further ECCS components (HPI and LPI).

The power distribution was obtained from core simulator results carried out for a typical German PWR (for beginning of cycle conditions, as they show the largest rod power factors). However, modelling of the entire number of fuel rods is still not feasible in ATHLET-CD (due to too long simulation time) and an appropriate averaging procedure was needed. As a compromise between accuracy and duration of the calculations, it was decided to model the fuel rods of each assembly by 4 representative rods, each representing one quartile of the assembly's rods (i.e. 75 rods), ordered by their rod power. For each quartile the average rod power factor (RPF) was calculated, which is shown by Fig. 4.4 with a maximum RPF = 1.567. According to the German guidelines for LOCA analyses, the most unfavorable conditions have to be selected. For the axial power density distribution, the most unfavorable power distribution is selected that the reactor protection system and assumed uncertainties allow, which is a distorted power profile with the maximum located in the upper part of the core (top-peaked power-profile). To implement that requirement, the RPFs derived from core simulator results have been multiplied by a generic top-peaked power profile that leads to a maximum linear heat generation rate (LHGR) of 455 W/cm in the current ATHLET-CD analyses. The value is slightly lower than the given LHGR verification value of 485 W/cm to be applied in conservative LOCA analysis (Wunderlich et al., 1990), but the latter could not be applied in the current analysis as it led to numerical problems during the start of the ATHLET-CD simulation. The power profiles are shown exemplarily by Fig. 4.5 for the assembly with maximum power.

The mechanical rod behavior module of ATHLET-CD calculates the thermal strains as well as the elastic and plastic deformations due to the difference between the rod internal pressure (RIP) and the system pressure. The RIP is dynamically calculated as a function of the mean gas-gap temperature and the gas-gap volume (including the fuel rod plenum volume) under consideration of the fuel porosity and the amount of gas substance (in moles). The amount of gas is calculated from the initial gas-gap volume, a given initial gas pressure and temperature, e.g. the fill gas pressure (which is 2.25 MPa for fresh Konvoi fuel (Wunderlich et al., 1990) at ambient temperature.

In case of fresh Konvoi fuel (low burn-up → 0.0 GWd/tHM), the steady state RIP of the maximum power rods is found to be between 6 and 7 MPa, as indicated by Fig. 4.6 (left side) and Fig. 4.7, which is in agreement to values reported by (Wunderlich et al., 1990). These values are the lowest steady state values, which can be observed for a fuel rod operated at that power level. With increasing operation time, i.e.

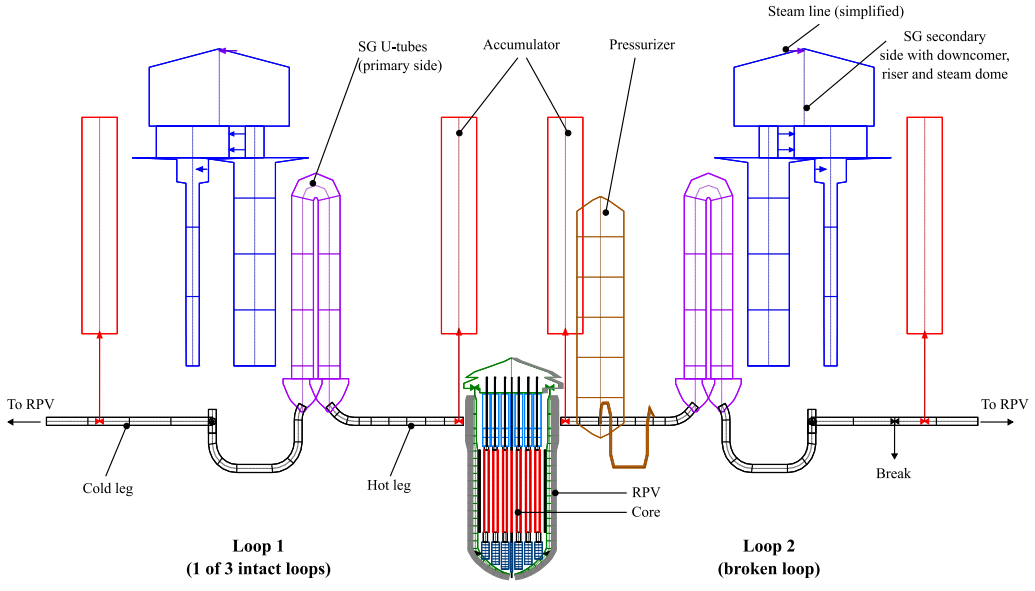

Fig. 4.3. Nodalization scheme of primary and secondary side.

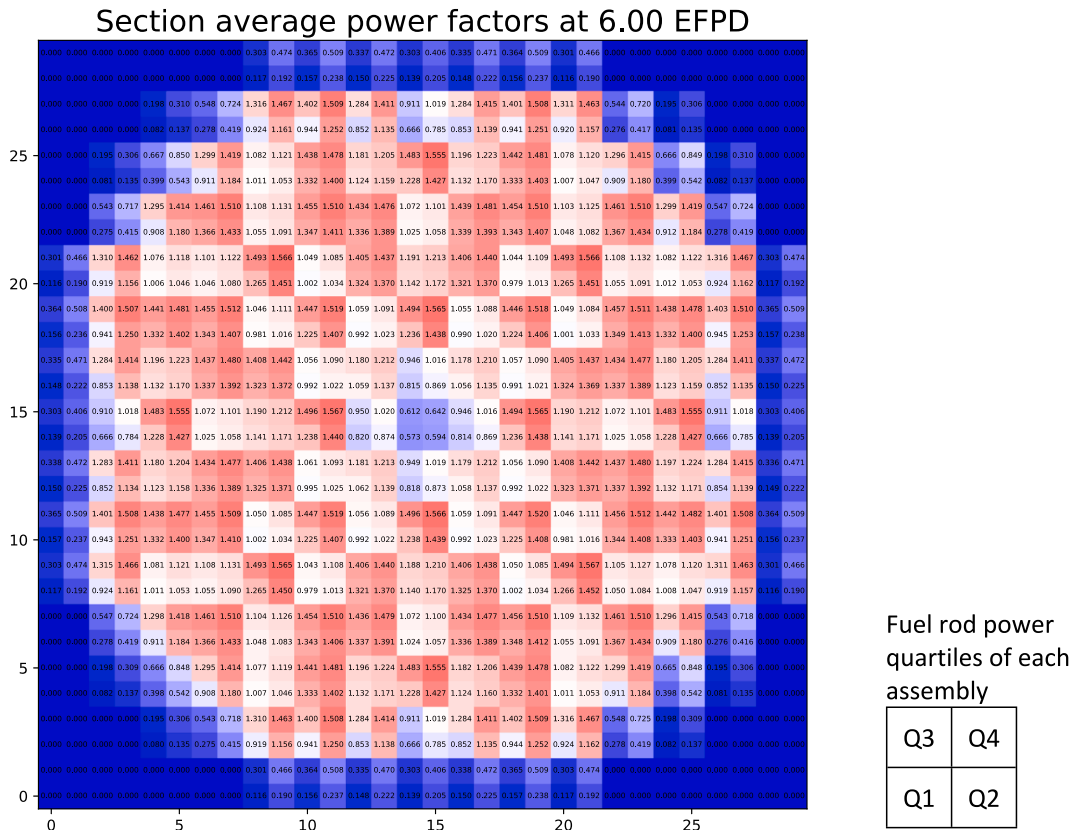

Fig. 4.4. Average rod power factors for 772 representative fuel rods (4 quartiles per assembly).

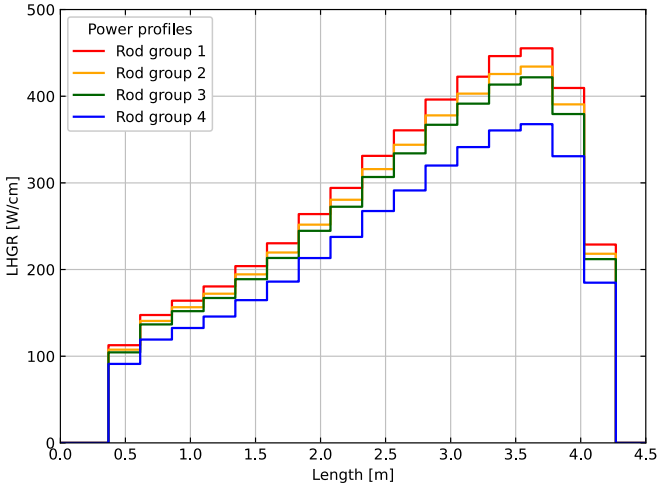

Fig. 4.5. Four top-peaked rod power profiles constructed for the assembly with maximum power.

increasing burn-up, the rods show higher RIP at the same power level because of the accumulation of fission gases in the gap. It is important to note that the accumulation of fission gas during normal operation is currently not computed by ATHLET-CD.

The current version of ATHLET-CD (version 3.3) allows the user to define only one global initial gas-gap pressure, which is applied across all 772 representative rods (core sections) as the initial value of the dynamically calculated RIP. There is, however, an alternative method within ATHLET-CD for simulating RIP evolution. This method permits a distinct initial pressure for each core section based on a globally rated value and adjusted according to a relative rod internal pressure scale. This approach requires user-provided (pre-calculated) tabulated functions of pressure evolution over time for each core section, but as these are not known beforehand, the method is typically impractical.

As a result, the current version of ATHLET-CD cannot accurately model the dependency of gas-gap pressure on burn-up at the onset of a LOCA transient. As a work-around, we have estimated a possible pressure range, starting from 2.25 MPa (cold-state gas-gap pressure for fresh fuel) to a conservatively high initial cold-state gas-gap pressure of 3.6 MPa (corresponding to the maximum rod-averaged burn-up of approx. 70 GWd/tHM observed at EOC). With the high initial pressure value, the simulations predict a maximum RIP of approximately 11.0 MPa under hot full power conditions (see the right side of Fig. 4.6), exceeding the conservative values reported in the literature (Wunderlich et al., 1990).

The simulations have been performed with both initial values. The first one returns the lower bound of the failed rod number and the second one returns the upper bound.

During the LB-LOCA, the system pressure drops within approx. 5 to 10 s from 15.8 MPa initial pressure down to values below 7.0 MPa (Fig. 4.7), which leads to a value of

$$\Delta p = p_{\mathrm{rod,int.}} - p_{\mathrm{sys}} > 0 \tag{1}$$

Afterwards, the system pressure is further reduced, while the rod internal pressure remains at a higher level for several seconds.

During the discharge phase of the LOCA transient, the peak cladding temperature (PCT) of the rods with highest heat generation rate reaches values of up to 1100 °C within approx. 5 s (see Section 4.4), which is a similar time span as it takes the system pressure to fall below $p_{\mathrm{rod,int.}}$. The maximum heating rates can exceed 400 K/s between 1 s and 2 s, followed by a more moderate heating rate of up to 100 K/s. Usually, a slight drop of the PCT is observed afterwards between 5 and approx. 20 s, followed by a another temperature rise to values above 1000 °C, with several rods that can reach values up to 1200 °C (depending on the investigated conditions, see the discussion in Section 4.4 and Fig. 4.17)

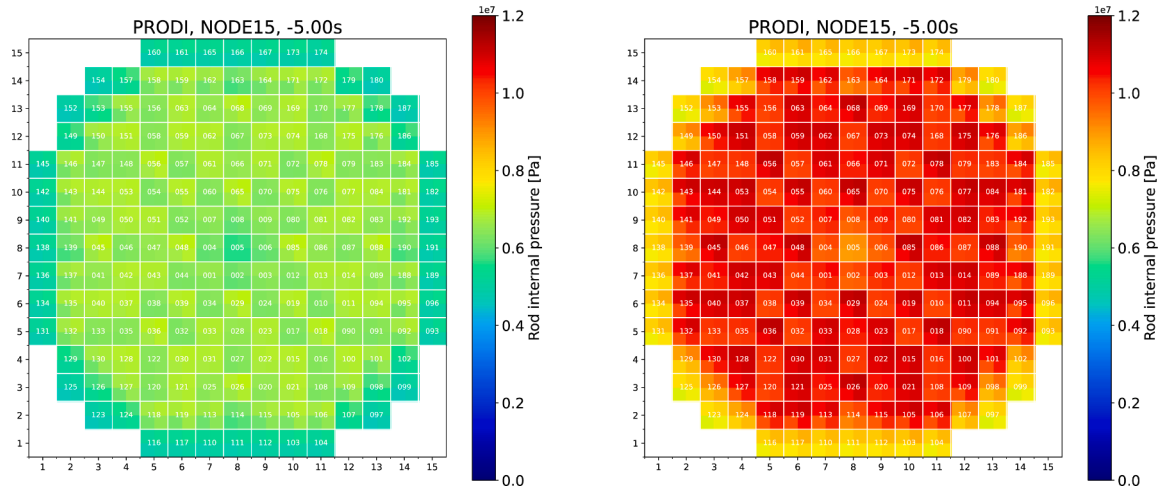

Fig. 4.6. Distribution of rod internal pressure PRODI calculated by ATHLET-CD for two bounding cases. Left side: initial pressure value 2.25 MPa applied for all rods (fresh fuel). Right side: initial pressure value 3.6 MPa applied for all rods.

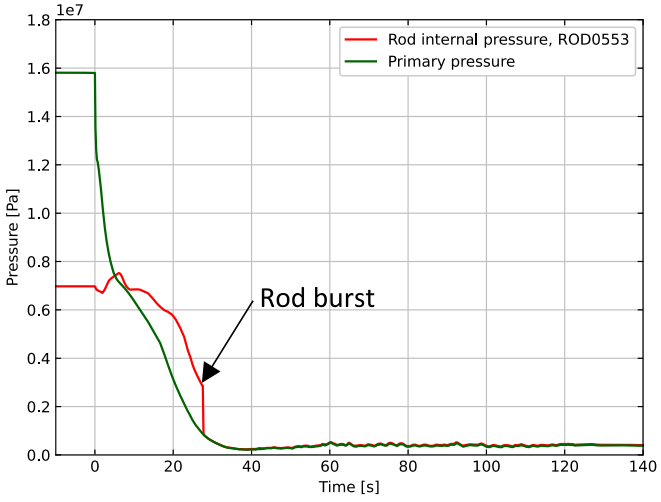

Fig. 4.7. Typical evolution of the primary pressure and RIP of high-power rod during the first 50 s of the LB-LOCA.

This second peak or plateau lasts until the rods are quenched by the ECCS (until approximately 80–120 s). Consequently, from about 10 s on, a significantly large internal overpressure is observed (can reach values in the order of 2.0 MPa, as shown by Fig. 4.7), while the cladding of those rods remains at high temperature. Consequently, deformation of the rods takes place, which is mainly caused by creep of the cladding material, which leads to ballooning and later to burst of rods. That process continues during the refilling and reflooding phases of the LB-LOCA as long as the rods are at elevated temperatures. Several correlations are implemented to model the creep behavior, which are based on similar assumptions. It is assumed that the deformation process up to burst of internally pressurized Zircaloy claddings can be calculated from the steady-state (secondary) creep equation of the material (Erbacher et al., 1982). The steady-state creep rate $\dot{\varepsilon}$ of a material at constant temperature and constant stress can be represented by a power law-Arrhenius equation (the so-called Norton equation) of the form:

$$\dot{\varepsilon} = \frac{d\varepsilon}{dt} = A\sigma^n \exp\left(-\frac{Q}{kT}\right) \tag{2}$$

σ is the applied hoop (azimuthal) stress in Pa, T is the cladding temperature given in K, and k is the universal gas constant = 8.314 J/mol·K^{-1}. The structure parameter A (unit MPa^{-n}·s^{-1}), the stress exponent n (dimensionless) and the activation energy Q (unit J/mol) are derived from experimental data. All implemented models assume symmetrical deformation of the rods. Therefore, the hoop stress for a tube under a differential pressure $\Delta p = p_{in} - p_{ex}$ is given by (Rill and Regensburg, 2017):

$$\sigma_h = \Delta p \frac{R}{s} - \frac{p_{in} + p_{ex}}{2} \tag{3}$$

with R as the instantaneous mean tube radius and s the instantaneous tube wall thickness.

Four different correlations for creep computation are implemented in the ATHLET-CD code, with separate correlations for hexagonal closed packed α-phase to the body centered cubic β-phase:

- Model based on Erbacher et al. (Erbacher et al., 1982);
- Model based on Rosinger et al. (Rosinger et al., 1979);
- Model of Burton (Burton et al., 1978) for α phase, but with a modified calculation procedure for the shear modulus G, as default and recommended option according to the ATHLET-CD manual (Lovasz et al., 2021). That correlation is called standard correlation of KESS (as it was used in the predecessor of ATHLET-CD, developed by IKE Stuttgart (Schatz and Hocke, 1995);
- Original model of Burton (Burton et al., 1978) for α phase.

It has to be mentioned, that no correlations are implemented in ATHLET-CD for the β-phase Zircaloy for Burton's models. For Erbacher and Rosinger correlations, the model parameters are given by Table 4.1. In case of the Erbacher correlation, the hoop stress is applied, while for the Rosinger correlation, the engineering stress is applied.

Table 4.1
Creep correlation parameters applied in ATHLET-CD for Erbacher and Rosinger model.

Model	Phase	n	A	Q
		–	MPa^{-n}·s^{-1}	J/mol
Erbacher et al. (Erbacher et al., 1982)	α phase	5.89	1487.0	321000 + 24.69 (T – 923.15)
	β phase	3.78	3.9721	141,919
Rosinger et al. (Rosinger et al., 1979)	α phase	5.32	2000.0	284,600
	β phase	3.79	8.1	142,300

The temperatures to describe both phases are implemented as:

$$\begin{array}{ll} T < T_\alpha = 1085.15\text{K} & \alpha\text{phase} \\ T_\alpha < T < T_\beta & \text{interpolation region} \\ T > T_\beta = 1248.15\text{K} & \beta\text{phase} \end{array} \quad (4)$$

The creep rates computed by the four different options are compared in Fig. 4.8 for the temperature range between 600 °C and 1100 °C and a stress range between 1.0 MPa and 100 MPa. Stress values up to 30 MPa are observed during the LOCA transient. Creep rates above 0.003/s have to occur to create large enough final strain of about 38 % (currently selected burst criterion) within the duration of 120 s (maximum observed time for quenching). Furthermore, the code limits the strain rate to a maximum value of 0.3/s in order to avoid too fast changes of geometry. This region of interest for the typical LOCA conditions is framed by the dashed lines in Fig. 4.8. It is visible that the Rosinger correlation produces significantly larger creep rates than the Erbacher model (approx. by a factor of two larger for the high temperature range, approx. one order of magnitude larger for the low temperature range). The Burton model gives similar values for the low-temperature α phase as the Rosinger correlation. Due to missing correlation for β phase in the ATHLET-CD implementation of the Burton model, the calculated creep rates for the high-temperature range are significantly lower than those computed by Rosinger as well as those by Erbacher. As the current status of the code is documented in this paper, the results of the Burton models shown in Fig. 4.8(c)-(d) are extended to whole temperature range (as it is done in the current version of the code).

The consequences of the four different creep models have been investigated for the rod with maximum power and the evolution of the hoop strain is depicted in Fig. 4.9. It can be seen that the Rosinger model leads to fastest straining of the cladding. It is the only model that leads to significant negative creep rates during the first temperature peak (during discharge phase, 3–4 s after break opening), with creep-down of the cladding to pellet and consequently $\varepsilon < 0$. Following the positive Δp after 10 s, the Rosinger model also leads to earliest start of ballooning of the cladding. However, the burst criterion (in this case 38 % maximum strain has been defined) is reached at almost the same time for all four models (2 s later for the Burton model compared to the Rosinger model). The evolution of the number of burst rods is shown by Fig. 4.10.[2] The Rosinger model results in a faster increase in the number of burst rods and also leads to a 20 % higher number of total burst rods compared to the other three burst models, and thus shows the most conservative results among the implemented creep models. Consequently, this model was applied to prepare the final analysis presented in Section 4.4.

Another important model parameter is the implemented rod burst criterion. ATHLET-CD provides four different rod burst models, which are discussed in (Taurines and Belon, 2022). For the current simulations, the maximum strain criterion has been selected, which is the simplest criterion Burst of rods is assumed as soon as the maximum hoop strain of the cladding reaches 38 %. This is slightly above the strain value reached when adjacent rods (assuming symmetric deformation and similar deformation of adjacent rods) get into contact (34 %).

4.3. Short description of the simulated accident scenario

For the investigated LB LOCA scenario, the reactor is operated at full power. To cover uncertainties of reactor power, the power is increased to 106 % of the nominal power in the current analysis (conservative value, 4187 MW). The LB-LOCA is initiated by a double-ended guillotine break of cold leg of Loop 2 (loop connected to the pressurizer, see Fig. 4.3), in combination with loss-of-offsite power (LOOP). The break is located close to the RPV with a break size of 2 x 4417 cm^2.

For DBA-LOCA, the assumptions for availability of the ECCS are made according to RSK guidelines and are summarized in Table 4.2. The single failure (SF) criterion is applied, which means that one hot leg injection train is blocked. Furthermore, maintenance (MA) of one accumulator has to be assumed. The accumulator and low-pressure injection pumps connected to the cold leg of the broken loop inject directly to the break (and are therefore not efficient). The active ECCS starts, when the emergency preparation signal is set. This signal is set, when two out of three of the following criteria are reached (activation by the reactor protection system):

- Pressure difference between containment and atmosphere > 30 mbar
- Primary pressure < 111 bar (absolute)
- Level in the pressurizer < 2.28 m

4.4. Numerical results

For the DBA-LBLOCA, two bounding cases were calculated, and the results are reported in the following. For the first simulation minimum initial RIP value was applied (2.25 MPa) while the second simulation was carried out with maximum initial RIP value (3.60 MPa).

At first, the simulation with minimum RIP is discussed. The maximum cladding temperatures of each of the 772 representative fuel rods observed during the LOCA, are depicted by Fig. 4.11. During the discharge phase a first temperature peak of 1124 °C (at 5.0 s) is found, which is mainly due to the stored energy in the fuel rods and almost complete loss of cooling (cladding temperatures approach fuel temperatures). A second peak is observed at approximately 12 s, followed by a reduction of PCT to 900 °C until approximately 20 s. At t = 5 s, the cladding temperature distribution is almost symmetrical within the core (Fig. 4.13). It has to be mentioned that in this figure, each FA is subdivided into 4 quadrants, and each quadrant indicates the temperature of one of the 4 representative rods (according to the power quartiles given by Fig. 4.4). Later at t = 20 s, a non-symmetrical temperature distribution is observed with reduced cladding temperature in the core quadrant which is located adjacent to the broken Loop 2 (Fig. 4.14). The emphasized temperature reduction in this area can be explained by the injection of the pressurizer inventory through hot leg of Loop 2 during this period of the accident and by an increased flow downwards into the direction of the break located at cold leg of Loop 2.

Injection from accumulators starts at 21 s, with support from active ECCS starting at 32 s, which leads to refilling of lower plenum and reflooding of the core starting from 50 s. Afterwards, more and more rods are quenched until approx. at 117 s all rods are quenched.

Due to the elevated temperature and a drop of the primary pressure below rod internal pressure at approx. 6 s after the beginning of the LOCA (see Fig. 4.7), the cladding of the first rods starts to balloon due to creep of the material. Fig. 4.12 shows the calculated strain for all nodes (772 representative rods times 18 nodes per rod). The deformation of cladding leads to reduction of the flow area between the fuel rods and reduces the coolability of those core sections, which are already at elevated temperature. Consequently, several representative rods heat up before they are quenched (third local peak of 1060 °C, which is still lower than the defined ECCS acceptance criterion of 1200 °C (von Linden et al., 2002).

At 26.9 s, the first rod reaches the specified burst criterion (38 % hoop strain). In total, 97 representative rods burst during the progression of the LOCA (corresponding to 7275 real fuel rods), which is equal to 12.6 % of the core. The nodes, which reach the burst criterion, are indicated in red color in Fig. 4.12. As the initial RIP value was set to its minimum (2.25 MPa), the calculated number of burst rods has to be understood as the lower limit of possible results. However, the acceptance criterion defined for German PWRs for the extent of core damage

[2] It has to be mentioned that the results discussed here with focus to influence of different creep models are not the same simulation case, which is shown in Section 4.4. The results presented here were obtained with high initial RIP and top-peaked power profile. For the final results in Section 4.4, several corrections of ECCS and decay heat have been implemented and thus lead to a slightly different final value of burst rods.

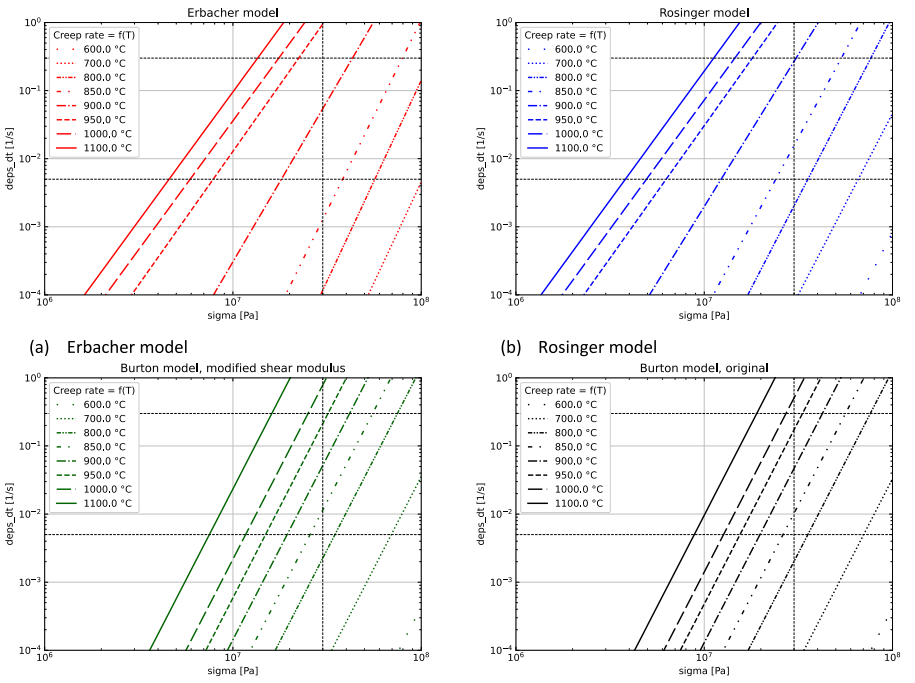

(a) Erbacher model

(b) Rosinger model

(c) Burton model (with modified shear modulus) as it is implemented in ATHLET-CD

(d) Burton model (original equations for shear modulus) as implemented in ATHLET-CD

Fig. 4.8. Creep rates calculated by the four creep rate models implemented in ATHLET-CD.

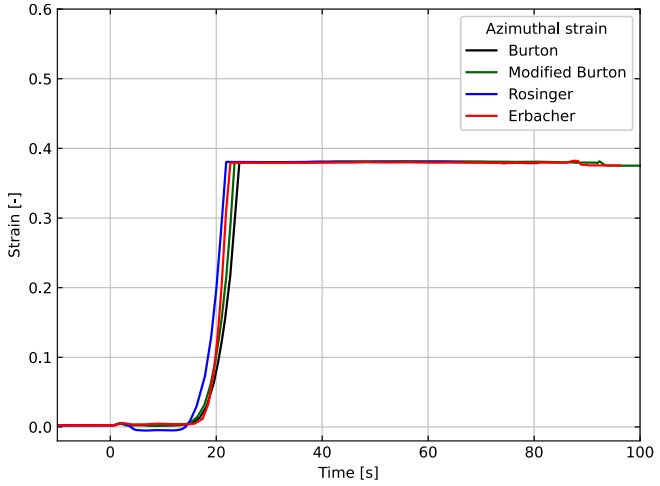

Fig. 4.9. Comparison of four creep rate models implemented in ATHLET-CD. Evolution of the (azimuthal) hoop strain of selected high power rod during LBLOCA.

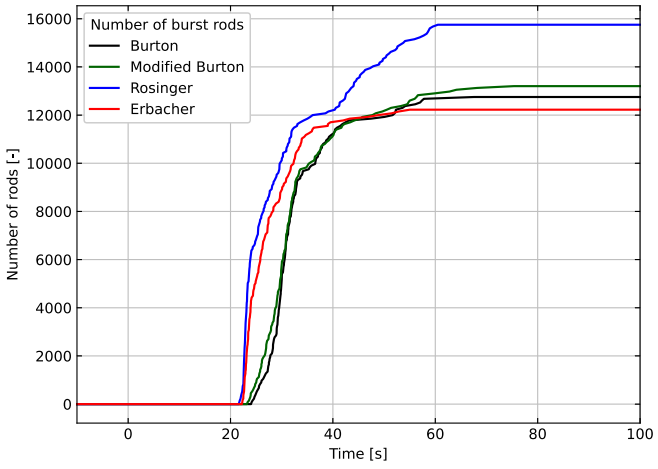

Fig. 4.10. Comparison of four creep rate models implemented in ATHLET-CD. Number of burst rods computed for a LB-LOCA case with top-peaked power profile.

is a maximum burst of 10 % of all rods (BMU, 2012) and this criterion is violated even by the lower limit of burst rods. The distribution of burst rods at the end of the LOCA transient is visualized by Fig. 4.15, and shows a strong correlation to the cladding temperature distribution at t = 20 s. Based on the deformation of the rods, a porosity factor is calculated for each CV of the core channels (Fig. 4.16).). This calculated porosity factor directly influences the flow cross-sectional area, and decreasing of porosity leads to decreasing flow cross-sections. This acts as a feedback parameter from the mechanical rod model to the thermohydraulic model, which leads to reduced coolability of the affected core regions.

A second simulation was performed with an increased initial RIP value, which was specified as 3.6 MPa (at ambient temperature). The corresponding max. RIP at hot full power conditions is 11.2 MPa

Table 4.2
Assumptions for the ECCS in the DBA LOCA scenario.

Injection System	Loop 1		Loop 2		Loop 3		Loop 4	
	HL	CL	HL	CL	HL	CL	HL	CL
Safety injection pumps (HPIS)	1	–	1	–	SF	–	1	–
Accumulators	1	1	1	1*	SF	1	MA	1
Low pressure injection pumps (LPIS)	1	1	1	1*	SF	1	1	1

1 Injection system available.
1* Injection system available, but injects to broken loop.
SF Not available due to single failure.
MA Not available due to maintenance.

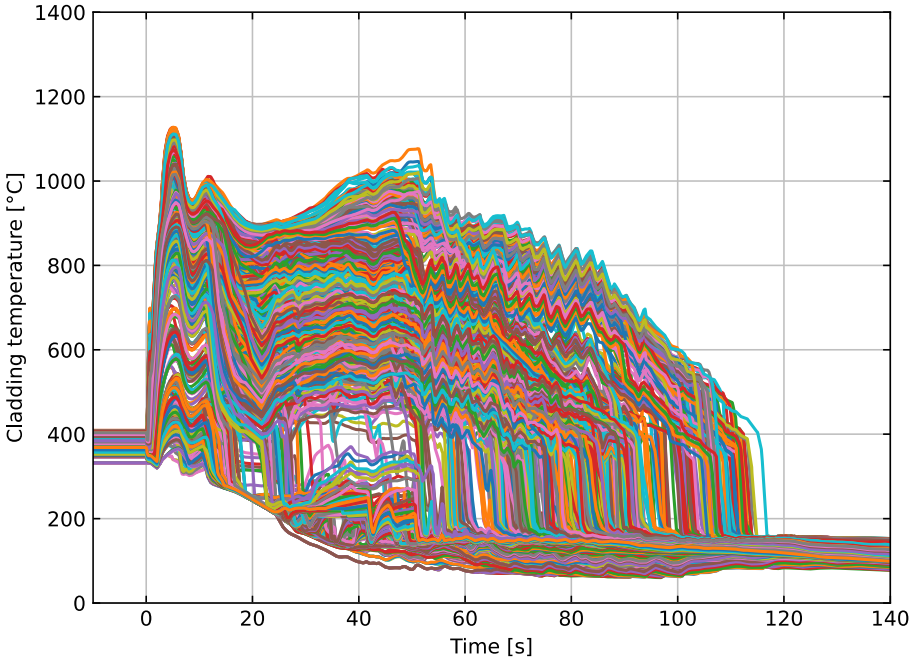

Fig. 4.11. Maximum cladding temperatures of 772 representative fuel rods.

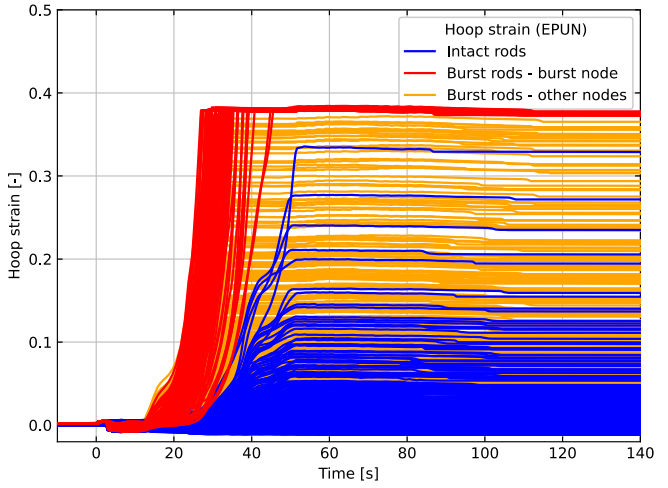

Fig. 4.12. Hoop strain of all 13,896 calculated cladding nodes, with 97 representative rods that reach the burst criterion (38 % hoop strain).

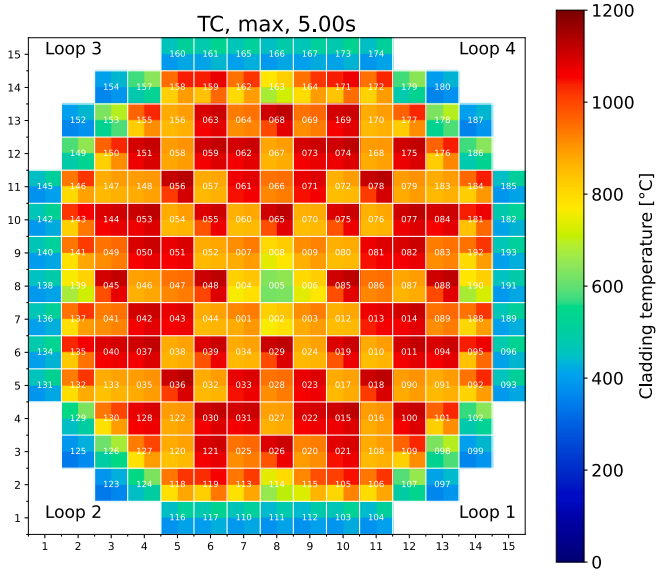

Fig. 4.13. Cladding temperature distribution within the core at t = 5 s.

(Fig. 4.6). As explained above, this value is considered as an overestimation of conservative values reported in literature (Wunderlich et al., 1990). From the results of the second simulation, it is observed that the cladding temperature of 5 representative rods (0.6 % of all rods) exceed 1200 °C, with a maximum of 1252 °C at 41.3 s (Fig. 4.17). Furthermore, an increased number of rods reach the burst criterion (225 representative rods, corresponding to 16,875 rods in the core, or 29.1 % of all rods, see Fig. 4.18). This value can be considered as the upper limit of the range of possible results.[3] If the real distribution of the RIP could be accounted for in the ATHLET-CD model, the number of burst fuel rods is expected to be in between the two limits.

[3] This holds under the assumption, that all other parameters are kept as specified in the simulation. In case of a complete uncertainty analysis (with all relevant input parameters are varied within their uncertainty range), an even higher number of burst rods might be obtained. The reader has to keep in mind that despite several important parameters have been selected conservatively (initial power, decay heat, power profile, rod internal pressure, and number of available ECCS systems), other parameters are specified at best estimate values (e.g. accumulator inventory, all ATHLET internal model parameters).

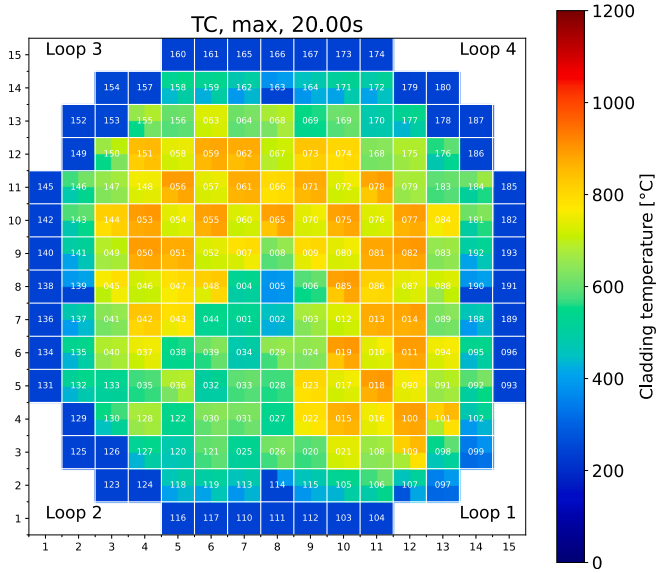

Fig. 4.14. Cladding temperature distribution within the core at t = 20 s.

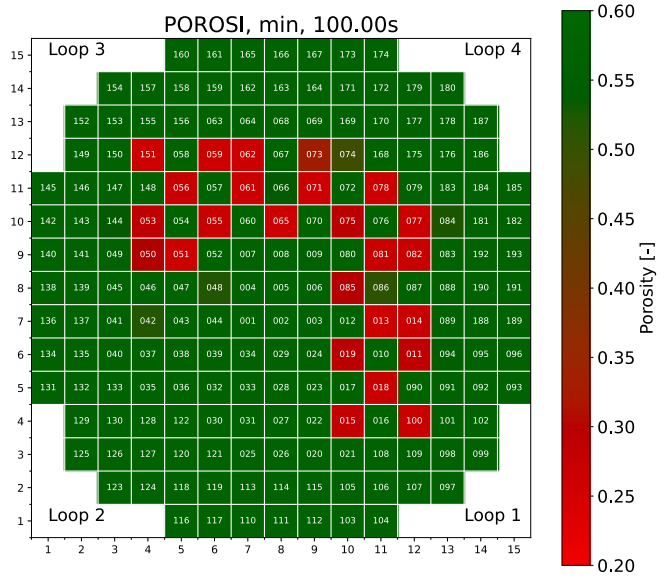

Fig. 4.16. Distribution of the porosity calculated within the core. For each core channel the minimum porosity is shown.

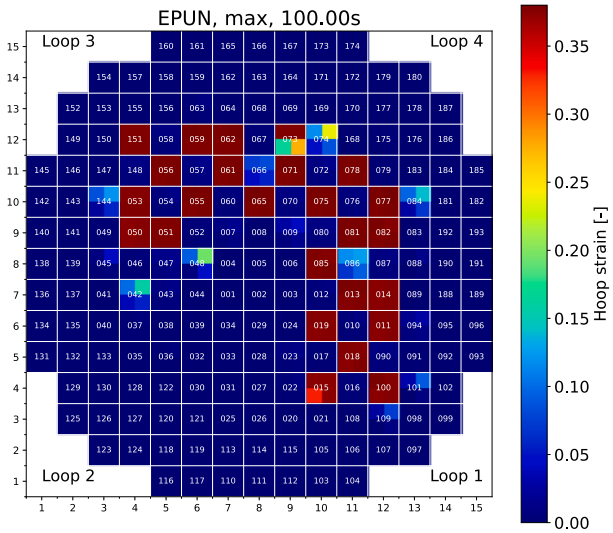

Fig. 4.15. Distribution of the maximum hoop strain at the end of the LOCA transient.

4.5. Discussion of ATHLET-CD results

In the frame of R2CA, HZDR developed a new approach to model the behavior of a PWR reactor under LOCA conditions. The model combines a 3D thermal hydraulic model of the RPV with the fuel rod model of ATHLET-CD and feedback from the fuel rod model back to the thermal–hydraulic model (based on calculation of reduction of the flow cross sectional areas). The model is integrated in a full plant ATHLET model of a four-loop PWR, which is able to take asymmetric thermal–hydraulic conditions into account, such as asymmetries that arise from break located only in 1 out of 4 loops, the injection of coolant from pressurizer or malfunction of one or several ECCS trains.

The 3D core model consists of 193 thermal–hydraulic channels (one per fuel assembly) and 772 representative fuel rods (4 representative fuel rods per fuel assembly) and is able to evaluate the local thermal–hydraulic response to a LB-LOCA for PWR. The fuel rod model estimates the rod internal pressure of each rod depending on initial RIP, temperature evolution and changes of geometry. Due to internal overpressure and elevated cladding temperatures, deformation of the cladding was observed with ballooning of hot rods that reach the defined burst criterion. In the current simulations, a maximum strain criterion (38 %) was implemented as the only burst criterion.

With the new approach, the number of burst rods (rod burst ratio) was estimated. However, the current version of ATHLET-CD has the shortcoming, that only a global initial value can be specified for dynamic calculation of the rod internal pressure, and this initial pressure value is applied to all representative fuel rods. Therefore, two bounding cases were calculated for the selected LB-LOCA scenario, with lower and upper limit of RIP and consequently lower and upper limit of RBR were obtained from the simulations. It is planned for a future release of ATHLET-CD to provide rod-specific initial values for the dynamic calculation of RIP.

One disadvantage of the newly developed approach is the very long computing time. Usually, 1 to 1.5 months CPU time were needed to reach 150 s of the LOCA with 2 CPU cores on a 3 GHz Intel Xeon CPU (where 1 CPU core is used for ATHLET/ATHLET-CD and the other one is used for NuT, a supplementary tool provided by GRS to improve calculation performance).

Despite the model still has several limitations and shortcomings, it is (to the author's knowledge) the first time that the system code ATHLET-CD was applied to model the degradation of fuel rods for a 3D configuration of a PWR core. In contrast to the coarse nodalization approaches applied previously with ATHLET-CD and other severe accident codes, the new approach enables to study the influence of local variations of the flow and cooling conditions and their consequences to the fuel rod behavior, and to predict the RBR more precisely.

As underlined in section 3.3, prediction of the number of burst rods should not be based on a single simulation run. Instead best-estimate plus uncertainty analysis should be carried out, as it was done for the assessment of other LOCA acceptance criteria (e.g. statistical assessment of peak cladding temperature performed by (Kozmenkov and Rohde, 2013; Kozmenkov and Rohde, 2014). Such method requires estimation of the assessment of uncertainties of all input parameters and a significantly increased computational effort. According to the Wilks theory, at least 93 repetitions of the simulation (with varied input parameters) are needed to quantify the two-sided tolerance limits of RBR with 95 %/95 % coverage/confidence level (Glaeser, 2008). Considering today's enhanced computational power and the high number of cores in typical workstation CPUs, HZDR should be able to conduct such statistical analyses using the new detailed core model in the coming months.

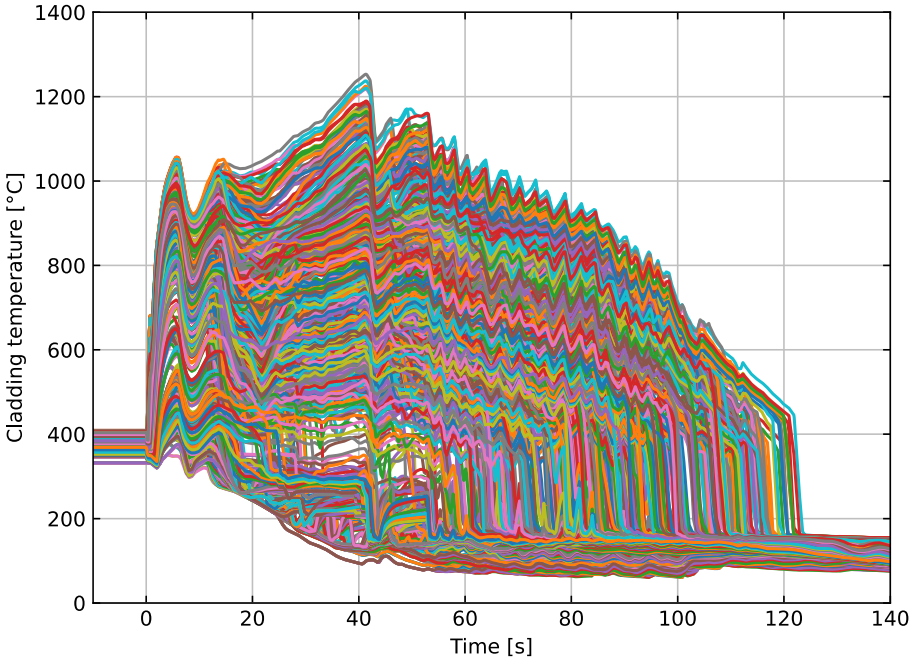

Fig. 4.17. Maximum cladding temperatures of 772 representative fuel rods.

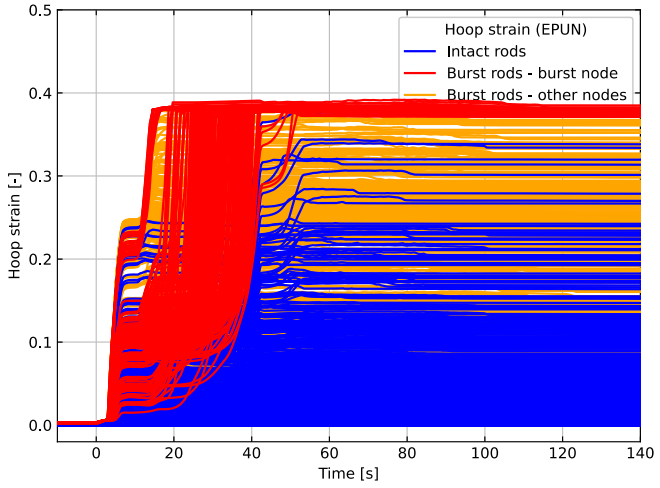

Fig. 4.18. Hoop strain of all 13,896 calculated cladding nodes, with 225 representative rods that reach the burst criterion (38 % hoop strain).

5. Summary of results and comparison of approaches

In the frame of the R2CA European project, specific efforts were focused on improving the simulation of loss-of-coolant accident on light water reactor with the objective to predict the rod burst ratio. Besides the approach consisting in a chain from a system thermalhydraulic code to a fuel performance code, approaches based on integral codes which couple thermal hydraulics and thermomechanical fuel rod behavior were investigated. These approaches allow feedback from fuel rod response on in-core flow such as the relation between deformation and flow section and the evolution of wall-to-fluid heat exchange surfaces. ENEA proposed an approach with the severe accident and source term code ASTEC. IRSN developed 3D core approach with the loss-of-coolant accident software DRACCAR. HZDR used the 3D version of the severe accident code ATHLET-CD to build 3D RPV PWR model. These approaches were illustrated by demonstrative applications representative of DBA: an intermediate break loss-of-coolant accident with ASTEC and DRACCAR and a large break loss-of coolant accident with ATHLET-CD. In addition, ENEA proposed an analysis of DEC-A accident conditions which exhibited higher peak cladding temperatures and then higher rod burst ratio than DBA case.

The new approaches proposed with these tools all aims at depicting the heterogeneous characteristics of the fuel rods composing a reactor core which can influence the rod thermomechanical response to the accident conditions and determine their burst potential. Therefore, simulations represent the different rods with respect to their power, location, rod internal pressure and characteristics associated to the fuel design. Distinct approaches were developed as it depends mainly on the capabilities of each code to model the core and the associated computational performance. ENEA proposed a PWR core description which is still based on a reduced number of core concentric thermalhydraulic channels (only 5) but with an increase of the number of equivalent fuel rods from 5 (1 per ring) to 20 selected according to the fuel assembly characteristics. On the other side, IRSN and HZDR proposed approaches which harness the 3D capabilities of DRACCAR and ATHLET-CD by modelling core thermal hydraulics with one channel per fuel assembly and allowing crossflow between fuel assembly channels. Each channel contains several equivalent fuel rods representing the fuel rod population composing each fuel assembly. IRSN and HZDR made two alternative choices, IRSN DRACCAR model reduces the 3D core domain to an eighth of the core and coupled it to multi-1D vessel plenums and downcomer. Such simplification highly reduces the computational cost of 3D core simulation in comparisons to a full core modelling. HZDR ATHLET-CD model uses a full 3D RPV model representing core, vessel plenums and downcomer in 3D proposing to deal with 3D flow in the whole vessel impacted by loop behavior asymmetry.

For some simulations, depending on the selection of burst criteria, burst is triggered on a maximum strain threshold value (set to 38 % in ATHLET-CD simulation and 40 % in ASTEC simulation). These values are not recommended as the selected strain threshold exceeds the limit strain corresponding to contact between rods for PWR core design. Indeed, the 2D (r,z) equivalent rod model used in these codes cannot represent with satisfactory such configuration and only 3D sub-channel modelling as the one proposed by DRACCAR can deal with it. Specific burst criteria developed for failed rod number prediction (Taurines et al., 2024) were tested on plant applications with ASTEC and

DRACCAR. Burst were not triggered on a maximum strain threshold when using R2CA burst temperature criteria. The predictions obtained with this criterion were compared to burst criteria classically used for core coolability demonstration in loss-of-coolant accident such as burst strain (NUREG-630) or burst stress criteria (EDGAR) or with true burst stress envelope proposed in R2CA (Taurines and Belon, 2022; Taurines et al., 2024). The comparisons showed that the choice of the burst criteria can strongly influence the prediction of the rod burst ratio. The R2CA burst temperature criterion which is close to the burst temperature proposed by Chapman (Powers and Meyer, 1980) lead to a higher burst ratio than the other criteria tested in DRACCAR simulations. In the case of ASTEC simulations, only the criterion corresponding to the lower envelope of the true burst stress proved to be more penalizing about number and timing of burst than the R2CA temperature criteria. To evaluate RBR, it's recommended to use at the same time, several burst criteria (stress, strain and temperature) in addition to this burst temperature criteria in order to cover the possible configurations and conditions which can exist in the core. Moreover, the predicted rod burst ratio should be considered with respect to the uncertainties associated to the burst criterion applied.

Even with 2D thermalhydraulic description, the increase of equivalent rod numbers when using ASTEC demonstrates a better description of the core response to LOCA. However, ENEA observes on the two scenarios that the average thermal hydraulics applied to the different equivalent rods plays a dominant role on their behavior and tends to homogenize their responses. Consequently, this observation tends to plead in favor the use of 3D core modelling. Indeed, the 3D approach using a single channel per fuel assembly connected in 3D to depict the core seems more able to represent the various responses of the fuel assemblies as highlighted by the heterogenous burst location obtained with DRACCAR and ATHLET-CD. Moreover, the use of several equivalent fuel rods to describe rod population among the fuel assembly can provide several fuel rod responses per fuel assembly which can be cumulated to evaluate the rod burst ratio.

In ATHLET-CD simulation, the use of 3D RPV model exhibited some 3D complex distribution of the hottest zone driven by 3D effects. This led to an asymmetric response of the core and location of burst rods in the core. The obtained result with this first 3D RPV application of ATHLET-CD for LOCA analysis seems to show that the evaluation of rod burst ratio in loss-of-coolant accident should rely on 3D RPV model due to the non-symmetric core response influenced by distinct behaviors of primary loops. Such conclusion should be confirmed by further application and with other simulation tools.

This work did not present how to handle the source term release and radiological consequences induced by burst of fuel rods during LOCA. However, these evaluations were at the center of concern in R2CA European project and specific demonstration of source term evaluation based on integral simulation were done for ASTEC and DRACCAR applications (Kaliatka, 2023). To do so, the ASTEC demonstrative cases run by ENEA benefits from the ASTEC severe accident modelling with description of phenomena associated to fission products and containment behavior. Consequently, ASTEC simulated in a whole sequence the LOCA transient, with fuel rod burst and the induced fission gas release, transport and chemistry in primary loops and containments. Besides IRSN proposed an automatic chain between DRACCAR and ASTEC code to evaluate containment behavior and source term release from fission gas release predicted at rod burst by DRACCAR. To ensure consistency in thermal hydraulics prediction within the chain, the same thermal-hydraulic code CESAR with the same nodalization of PWR loops is used in DRACCAR and ASTEC applications. Concerning HZDR evaluation, the source term released to environment was evaluated analytically based on coarse assumptions as no specific tools or model was chained or coupled to ATHLET-CD simulations.

It's reminded that simulation presented in this work corresponds to demonstrative cases and therefore, the results cannot be directly used to draw conclusions for safety demonstration of PWR. Nevertheless, through this work, recommendations for failed rod number prediction by PWR LOCA simulation can be proposed. The use of realistic core description is encouraged and in particular the development of 3D core model using several fuel rod objects per fuel assemblies. According to the current challenge set by burst prediction, it seems difficult to select an accurate burst criterion and alternatively several burst criteria or conservative envelopes should be used as the one proposed in the R2CA project (Taurines et al., 2024). Finally, the approach for failed rod number evaluation should manage uncertainties and in particular the one associated to reflooding and thermal hydraulics phenomena or to clad ballooning and burst.

6. Conclusions and prospects on LOCA simulations for RBR evaluation in support to ST evaluation

The work presented in this paper, devoted to rod burst ratio evaluation in loss-of-coolant accident, encourages the development of advanced core modelling with 3D thermalhydraulic model coupled to thermomechanical fuel rod model. It was demonstrated that the status of integral codes (DRACCAR, ATHLET-CD) allows to depict each fuel assembly with several 2D (r,z) lumped rods associated to an average fuel assembly thermal hydraulics resolved within a 3D core model. Moreover, the response obtained with ATHLET-CD full 3D RPV showed an influence of complex 3D flow distribution on rod responses. As the maturity of 3D thermalhydraulic system code allows now the modelling of many complex situation and as the tools still continue to progress with respect to their improvements on validation (Herer, 2023), it could be expected in a near future some advances on methodologies with the use of 3D core modelling able to evaluate more realistically the rod burst ratio with an increased number of modelled fuel rods.

Whatever the core model used, this work reminds that the evaluation of the rod burst ratio is strongly dependent to the burst criteria which are selected. The use of criteria specific to the failed rod number evaluation are recommended such as the ones that were developed in the frame of the R2CA European project. Actually, the evaluation of the rod burst ratio should incorporate simulation in a global methodology which should account for the various uncertainties on inputs or models and in particular on burst criteria and on thermal hydraulics prediction. This management could be inspired by the best-estimate plus uncertainties approaches in use for the core coolability assessment in LOCA conditions.

Finally, this work shows the status of RBR evaluation for the three codes. It also helps to identify possible improvements of the software to update the proposed methods. For instance, one modification in ATHLET-CD could be to allow different rod internal pressures to fuel rods and chain application to fission transport and chemistry models. Concerning ASTEC and DRACCAR, one possible improvement could be brought to ISODOP module which manage fission product initial inventory and decay. Currently this module is based on an average core fission product inventory which is proportionally distributed with rod power factor whereas it could be relevant to set particularized fission products inventory respective to each fuel rods depending on burn-up and fuel types.

Further updates of RBR simulation with refined core model probably require an increase of the number of representative rods and associated thermal hydraulics channels. In parallel, validation of 3D core and RPV model must be pursued. Moreover, some efforts should be required to reduce computational cost of 3D thermal hydraulics resolution. Such reduction could feed opportunities to introduce 3D RPV model within integral severe accident code able to evaluate LOCA transient from initiator to source term release in the environment. If the status of the developed approaches still needs to be strengthened, their development is pursued due to the possible outcomes for PWR safety assessment or to study the influence on source term of new fuel rod design, mitigation system or plant modification.

Declaration of competing interest

The authors declare that they have no known competing financial interests or personal relationships that could have appeared to influence the work reported in this paper.

Acknowledgement funding

This project has received funding from the Euratom research and training programme 2014-2018 under grant agreement No 847656.

.

Disclaimer

Views and opinions expressed in this paper reflect only the author's view and the European Commission is not responsible for any use that may be made of the information it contains.

Acknowledgement

Authors specifically thanks the R2CA project leader Nathalie GIRAULT from IRSN for the advice on writing and the review of this article.

References

Martina Adorni, Alessandro Del Nevo, Francesco D'Auria, Oscar Mazzantini, "A Procedure to Address the Fuel Rod Failures during LB-LOCA Transient in Atucha-2 NPP", Science and Technology of Nuclear Installations, vol. 2011, Article ID 929358, 11 pages, 2011. https://doi.org/10.1155/2011/929358.

Arkoma, A., Hänninen, M., Rantamäki, K., Kurki, J., Hämäläinen, A., 2015. Statistical analysis of fuel failures in large break loss-of-coolant accident (LBLOCA) in EPR type nuclear power plant. Nucl. Eng. Des. 285, 1–14. https://doi.org/10.1016/j.nucengdes.2014.12.023.

Austregesilo, H., Schöffel, P., von der Cron, D., Weyermann, F., Wielenberg, A., and Wong, K.W., ATHLET 3.3 User's Manual, GRS-P-1/Vol.1 Rev. 9. 2021, Gesellschaft für Anlagen- und Reaktorsicherheit (GRS) gGmbH.

Baccou, J., Zhang, J., Fillion, P., Damblin, G., Petruzzi, A., Mendizábal, R., Takeda, T., 2019. Development of good practice guidance for quantification of thermal-hydraulic code model input uncertainty. Nucl. Eng. Des. 110173 https://doi.org/10.1016/j.nucengdes.2019.110173.

Balay, S., Abhyankar, S., Adams, M., Benson, S., Brown, J., Brune, P., . . . Kaushik, D. (s. d.). PETSc Web page. Taken from https://petsc.org/.

BMU, RS-Handbuch, 3-0.1, Sicherheitsanforderungen an Kernkraftwerke vom 22. November 2012, Neufassung vom 3. März 2015. 2015, Bundesministerium für Umwelt, Naturschutz, Bau und Reaktorsicherheit.

Burton, B., Donaldson, A.T., Reynolds, G.L., 1978. Interaction of Oxidation and Creep in Zircaloy-2, in Zirconium in the Nuclear Industry. ASTM International.

Capps, N., Wysocki, A., Godfrey, A., Collins, B., Sweet, R., Brown, N., Lee, S., Szewczyk, N., Hoxie-Key, S., 2021. Full core LOCA safety analysis for a PWR containing high burnup fuel. Nucl. Eng. Des. 379, 111194 https://doi.org/10.1016/j.nucengdes.2021.111194.

Chailan, L., Bosland, L., Carénini, L., Chambarel, J., Cousin, F., Chatelard, P., Drai, P., Kioseyian, G., Phoudiah, S., Topin, V., 2019. "Overview of ASTEC integral code status and perspectives", *The nineth European Review Meeting on Severe Accident Research (ERMSAR2019)*. Czech Republic, Prague. Retrieved from https://irsn.hal.science/irsn-04106726.

Chapman, R.H., 1979. Multi-rod Burst Test. Oak Ridge National Laboratory. Program Progress report April-June 1979 USNRC report – ORNL/NUREG/CR-1023,.

Chatelard, P., et al., 2016. Main modelling features of ASTEC v2.1 major version. Ann. Nucl. Energy 93, 83–93. https://doi.org/10.1016/j.anucene.2015.12.026.

Chatelard, P. et al., "D40.45 – Set of final reference NPP ASTEC input decks", Report of EU-CESAM project, 2017.

Diaz-Pescador, E., Grahn, A., Kliem, S., Schäfer, F., Höhne, T., 2020. Advanced modelling of complex boron dilution transients in PWRs - Validation of ATHLET 3D-Module against the experiment ROCOM E2.3. Nucl. Eng. Des. 367.

Diaz-Pescador, E., Schäfer, F., Kliem, S., 2021. Modelling of multidimensional effects in thermal-hydraulic system codes under asymmetric flow conditions-Simulation of ROCOM tests 1.1 and 2.1 with ATHLET 3D-Module. Nucl. Eng. Technol. 53 (10), 3182–3195.

Herer, C., 2023. CSNI status report "3D capabilities of thermalhydraulic system codes": Lessons learned, Nuclear Engineering and Design, Volume 405, ISSN 0029-5493, https://doi.org/10.1016/j.nucengdes.2023.112188.

Diaz-Pescador, E., Thesis (Ongoing work). 2023.

E.ON, *Kernkraftwerk Isar 2. Abschlussbericht für den Europäischen Stresstest.* 2011.

Erbacher, F.J., Neitzel, H.J., Rosinger, H.E., Schmidt, H., and Wiehr, K., Burst criterion of Zircaloy Fuel Claddings in a Loss-of-Coolant Accident, in Zirconium in the Nuclear Industry; Fifth Conference, ASTM STP 754, D.G. Franklin, Editor. 1982, American Society for Testing and Materials. p. 271-283.

Geelhood, K.J., Luscher, W.G., Raynaud, P.A., Porter, I.E., 2015. A computer code for the calculation of Steady-State, thermal-mechanical behavior of oxide fuel rods for high burnup. – Report PNNL-19418 Vol. 1 Rev.2.

Glaeser, H., 2008. GRS method for uncertainty and sensitivity evaluation of code results and applications. Sci. Technol. Nuclear Install. 2008.

Glantz, T., Taurines, T., De Luze, O., Belon, S., Guillard, G., Jacq, F., 2018. DRACCAR: A multi-physics code for computational analysis of multi-rod ballooning, coolability and fuel relocation during LOCA transients Part one: General modelling description. Nucl. Eng. Des. 339, 269–285. https://doi.org/10.1016/j.nucengdes.2018.06.022.

International Atomic Energy Agency. Vienna, (2016), "Safety of nuclear power plants: design", International Atomic Energy Agency report no. SSR-2/1 (Rev. 1), pp. 23-24, IAEA safety standards series, IAEAL 16-01014, ISBN 978–92–0–109315–8.

Kaliatka T. (LEI), Berezhnyi A., Krushynskyy A., Sholomitsky S. (ARB), Bousbia A., Malkhasyan A. (Bel V), Müllner N., Zimmer R. (BOKU), Herranz L. E., Iglesias R. (CIEMAT), Ederli S., Mascari F. (ENEA), Jobst M. (HZDR), Belon S., Dieschbourg K., Girault N., Kremer F., Obada O. (IRSN), Hózer Z., Kulacsy K. (EK), Gumenyuk D. (SSTC-NRS), Foucaud P. (TRACTEBEL), Kecek A., Klouzal J., Kral P. (UJV-NRI), Arkoma A., Marton S. (VTT), (2023). "Reassessment of reactor tests cases" - Final report D2.7 - R2CA H2020 EU project.

Kozmenkov, Y., Rohde, U., 2013. Application of statistical uncertainty and sensitivity evaluations to a PWR LBLOCA analysis calculated with the code ATHLET. Part 1: uncertainty analysis. Kerntechnik 78 (4), 354–361.

Kozmenkov, Y., Rohde, U., 2014. Application of the method for uncertainty and sensitivity evaluation to results of PWR LBLOCA analysis calculated with the code ATHLET Part 2: sensitivity analysis. Kerntechnik 79 (2), 97–102.

L. Lovasz S. Weber M.K. Koch Simulation of Asymmetric Severe Accidents Using the Code System AC2 2018 Berlin.

L. Lovasz S. Weber M.K. Koch Investigation of the Effect of the Spent Fuel Pool Configuration on Fuel Degradation 2019 Praha, Czech Republic.

Lovasz, L., Austregesilo, H., Bals, C., Hollands, T., Köllein, C., Luther, W., Pandazis, P., Schubert, J.D., Tiborcz, L., Weber, S., and Wielenberg, A., ATHLET-CD 3.3 User's Manual, GRS-P-4/Vol. 1 Rev. 8. 2021, Ges. für Anlagen- und Reaktorsicherheit (GRS).

Lovász, L., Bals, C., D'Alessandro, C., Hollands, T., Köllein, C., Austregesilo, H., Pandazis, P., Tiborcz, L., and Weber, S., ATHLET-CD Mod 3.3 Models and Methods, GRS-P-4/Vol.2 Rev. 0. 2021, Gesellschaft für Anlagen- und Reaktorsicherheit (GRS) gGmbH.

Lovasz, L., Weber, S., Koch, M.K., 2018. Comparison of a Hypothetical Strongly Asymmetrical Severe Accident Using the Standard and the New Nodalization Method with the Code System AC. 27th International Conference Nucelar Energy for New Europe (NENE). Portoroz.

Montgomery, R., Norris, R.N., 2019. Measurements and modelling of the gas permeability of high burn-up pressurized reactor fuel rods. J. Nucl. Mater. 523, 206–215. https://doi.org/10.1016/j.jnucmat.2019.05.041.

Neeb, K.-H., 1997. The radiochemistry of nuclear power plants with light water reactors. Walter de Gruyter.

Nowack, H., Chatelard, P., Chailan, L., Hermsmeyer, S.t., Sanchez, V., Herranz, L., 2018. CESAM – Code for European Severe Accident Management, EURATOM Project on ASTEC Improvement. Ann. Nucl. Energy 116, 128–136. https://doi.org/10.1016/j.anucene.2018.02.021.

Pandazis, P., Ceuca, S.C., Schöffel, P., and Hristov, H.V., Investigation of Multidimensional flow mixing phenomena in the reactor pressure vessel with the system code ATHLET, in Nureth-16. 2015. p. 3378-3391.

Pettersson, K., et al., 2009. "Nuclear Fuel Behaviour in Loss-of-coolant Accident (LOCA) Conditions. OECD-NEA, Paris, France, p. 369. State-of-the-art-report", in,.

Pointer, W., Berner, N., Kloos, M., Wenzel, S., 2018. Gesellschaft für Anlagen- und Reaktorsicherheit (GRS) gGmbH. Statistische LOCA-Analysen, GRS-519.

Powers, D.A. and Meyer, R.O., "Cladding swelling and rupture models for LOCA analysis", Technical Report NUREG-630, 1980.

Reduction of Radiological Consequences of Design Basis Accident and design extension accidents, R2CA Project H2020, CORDIS European Commission website, https://cordis.europa.eu/project/id/847656.

Rill, G., 2017. Technische Mechanik II, Lecture Notes.

Rosinger, H.E., Bera, P.C., Clendening, W.R., 1979. Steady-State Creep of Zircaloy-4 Fuel Cladding from 940-K to 1873-K. J. Nucl. Mater. 82 (2), 286–297.

Schatz, A., Hocke, K.D., 1995. Kess - a Modular Program System to Simulate and Analyze Core Melt Accidents in Light-Water Reactors. Nucl. Eng. Des. 157 (1–2), 269–280.

Schöffel, P., Entwicklung eines ATHLET-internen 2D/3D-Moduls, TN-SCO-01/11. 2011, Gesellschaft für Anlagen- und Reaktorsicherheit (GRS) mbH.

Stephenson, W., Dutton, L.C., Handy, B.J., Smedley, C., 1991. "Realistic methods for calculating the releases and consequences of a large LOCA", Report EUR 14179EN - Commission of the European Communities - Nuclear Science and Technology - ISBN 92-826-4632-7. Office for Official Publications of the European Communities, Brussels, p. 1992.

Taurines, T., Belon, S. (IRSN), Arkoma, A. (VTT), Kaliatka, T. (LEI), Kulacsy, K. (EK), Jobst, M. (HZDR), Ovdiienko, I. (SSTC), Van Uffelen, P. (JRC), Klouzal, J. (UJV), Calabrese, R. (ENEA), (2022). "Rod cladding failure during LOCA - Experimental

database reassessment and model and code improvements" - Final report D3.4 - R2CA H2020 EU project.

Taurines, T., Belon, S. (IRSN), Arkoma, A. (VTT), Kaliatka, T. (LEI), Kulacsy, K. (EK), Jobst, M. (HZDR), Ovdiienko, I. (SSTC), Van Uffelen, P. (JRC), Klouzal, J. (UJV), Calabrese, R. (ENEA), (2023). "Rod cladding failure during LOCA - Progress report on experimental database reassessment and on model and code improvements" - D3.3 report - H2020 EU R2CA project.

Taurines, T., Glantz, T., Belon, S., Kulacsy, K., Király, K., Nagy, R., Szabó, P., Dif, B., Arkoma, A., 2024. New Burst Criteria for Loss Of Coolant Accidents Radiological Consequences Assessment. Ann. Nucl. Energy 206, 110646. https://doi.org/10.1016/j.anucene.2024.110646.

von Linden, J., Löffler, H., Müller-Ecker, D., Verstegen, C., and Köberlein, K., Assessment of the Accidental Risk of Advanced Pressurized Water Reactors in Germany, GRS-184. 2002.

Wielenberg, L., Lovasz, P., Pandazis, A., Papukchiev, L., Tiborcz, P.J., Schöffel, C., Spengler, M., Sonnenkalb, A., 2019. Schaffrath: Recent improvements in the system code package AC2 2019 for the safety analysis of nuclear reactors. Nucl. Eng. Des. 354 https://doi.org/10.1016/j.nucengdes.2019.110211.

Wunderlich, F., Eberle, R., Gärtner, M., and Groß, H., Brennstäbe von Leichtwasserreaktoren. KTG-Seminar, ed. Kerntechnische Gesellschaft e.V. 1990, Köln: Verlag TÜV Rheinland.

Yamate, K., Mori, M., Ushio, T., Kawamura, M., 1997. Design of a gadolinia bearing mixed-oxide fuel assembly for pressurized water reactors. Nucl. Eng. Des. 170 (1–3), 35–51. https://doi.org/10.1016/S0029-5493(97)00010-1.

Ziegler, A., Allelein, H.J., Reaktortechnik: Physikalisch-technische Grundlagen. 2nd, Berlin 2013 Springer Heidelberg.